



**HAL**  
open science

# Synthesis of new halogenated flavonoid-based isoxazoles: in vitro and in silico evaluation of $\alpha$ -amylase inhibitory potential, a SAR analysis and DFT studies

Ilyes Saidi, Marwa Manachou, Mansour Znati, Jalloul Bouajila, Hichem Ben  
Jannet

## ► To cite this version:

Ilyes Saidi, Marwa Manachou, Mansour Znati, Jalloul Bouajila, Hichem Ben Jannet. Synthesis of new halogenated flavonoid-based isoxazoles: in vitro and in silico evaluation of  $\alpha$ -amylase inhibitory potential, a SAR analysis and DFT studies. *Journal of Molecular Structure*, 2022, 1247, pp.131379. 10.1016/j.molstruc.2021.131379 . hal-04755058

**HAL Id: hal-04755058**

**<https://hal.science/hal-04755058v1>**

Submitted on 13 Nov 2024

**HAL** is a multi-disciplinary open access archive for the deposit and dissemination of scientific research documents, whether they are published or not. The documents may come from teaching and research institutions in France or abroad, or from public or private research centers.

L'archive ouverte pluridisciplinaire **HAL**, est destinée au dépôt et à la diffusion de documents scientifiques de niveau recherche, publiés ou non, émanant des établissements d'enseignement et de recherche français ou étrangers, des laboratoires publics ou privés.



Distributed under a Creative Commons Attribution - NonCommercial 4.0 International License

1 **Synthesis of new halogenated flavonoid-based isoxazoles: *in vitro* and *in silico***  
2 **evaluation of  $\alpha$ -amylase inhibitory potential, a SAR analysis and DFT studies**

3

4 Ilyes Saidi<sup>a</sup>, Marwa Manachou<sup>b</sup>, Mansour Znati<sup>a</sup>, Jalloul Bouajila<sup>c\*</sup>, Hichem Ben Jannet<sup>a,\*</sup>

5 <sup>a</sup> University of Monastir, Faculty of Sciences of Monastir, Department of Chemistry, Laboratory of  
6 Heterocyclic Chemistry, Natural Products and Reactivity (LR11ES39), Team: Medicinal Chemistry  
7 and Natural Products, Avenue of Environment, 5019 Monastir, Tunisia

8 <sup>b</sup> University of Tunis El Manar, Faculty of Sciences of Tunis, Department of Chemistry, Research  
9 Laboratory Characterization, Applications and Modeling of Materials, LCAMM, 2092, Tunis,  
10 Tunisia

11 <sup>c</sup> Laboratoire de Génie Chimique, Université de Toulouse, CNRS, INPT, UPS, Toulouse, France.

12 \***Corresponding authors:** hichem.bjannet@gmail.com (H.B.J.) jalloul.bouajila@univ-tlse3.fr (J.B)

13

14 **ORCID**

15 Ilyes SAIDI ID <https://orcid.org/0000-0002-6408-1482>

16 Mansour Znati ID <http://orcid.org/0000-0002-4234-8043>

17 Jalloul Bouajila ID <https://orcid.org/0000-0002-2439-5145>

18 Hichem Ben Jannet ID <https://orcid.org/0000-0001-5858-1803>

19

20

21 **Abstract**

22 Carbohydrates are the main source of calories in most diets, and  $\alpha$ -amylase is considered one of the  
23 main enzymes that initiate their digestion. The inhibition of  $\alpha$ -amylase is therefore considered to be  
24 a therapeutic strategy for the treatment of disorders of glucose absorption, such as dental caries,  
25 periodontal disease, overweight, obesity and diabetes. On the other hand, flavonoids, isoxazoles and

26 halogenated derivatives are of great interest in medicinal chemistry due to their considerable  
27 bioactivities. Therefore, this work describes the design, the synthesis and the  $\alpha$ -amylase inhibitory  
28 potential of new halogenated flavonoid-based isoxazoles, and their biological properties. In fact, the  
29 condensation of a previously synthesized halogenated flavonol with different aryl nitrile oxides  
30 afford thirteen new hybrid cycloadducts (**2a-m**). Their structures were characterized by  $^1\text{H}$  NMR,  
31  $^{13}\text{C}$  NMR and HRMS analysis. The physicochemical properties of these compounds (**2a-m**) were  
32 also evaluated. The newly synthesized cycloadducts were evaluated *in vitro* for their  $\alpha$ -amylase  
33 inhibitory activity and excellent results were noted. The compound **2b** ( $\text{IC}_{50} = 16.2 \pm 0.3 \mu\text{M}$ )  
34 exhibited the highest anti- $\alpha$ -amylase activity comparable to that of the standard substance  
35 (Acarbose,  $\text{IC}_{50} = 15.7 \pm 0.2 \mu\text{M}$ ). The study of the Structure-Activity Relationship (SAR) was  
36 sufficiently discussed based on the Molecular Docking analysis and the Density Functional Theory  
37 (DFT) studies.

38

39 **Keywords:** Flavonoid-based isoxazoles, Cycloaddition, DFT study,  $\alpha$ -Amylase inhibition,  
40 Molecular docking, SAR analysis.

41

## 42 **1. Introduction**

43 Diabetes mellitus and overweight, although being non-communicable diseases, constitute a major  
44 public health problem around the world [1-2]. On the other hand, carbohydrates are known as the  
45 main source of calories in most diets. Therefore, inhibiting the digestion of foods rich in  
46 carbohydrates and blocking the absorption of monosaccharides can decrease the intake of calories,  
47 which promotes the weight loss and the fight against obesity [3]. In addition, the succession of  
48 carbohydrate consumption leads to postprandial hyperglycemia in diabetic subjects [4-5]. Diabetes  
49 mellitus is primarily typified by uncontrolled blood sugar levels [3,6]. Thus, inhibiting carbohydrate  
50 breakdown implements a fundamental strategy to control diabetes.

51 Furthermore,  $\alpha$ -amylase ( $\alpha$ -1,4-glucan-4-glucanohydrolase, EC.3.2.1.1) is an enzyme which has  
52 the most important contribution to start the digestion of carbohydrates [7-8]. Indeed,  $\alpha$ -amylase is a  
53 digestive enzyme which hydrolyzes  $\alpha$ -1,4-glycosidic bonds of carbohydrates, such as glycogen,  
54 starches and other polysaccharides, to generate oligosaccharides of variable length capable of being  
55 hydrolyzed by other digestive enzymes into monosaccharides which can be absorbed by cells [7-8].  
56  $\alpha$ -Amylase inhibitors reduce the glycemic index by delaying the hydrolysis of carbohydrates. The  
57 inhibition of  $\alpha$ -amylase enzyme, leading to a drop in blood glucose levels, is considered a  
58 therapeutic strategy for the treatment of carbohydrate absorption disorders, such as dental caries,  
59 periodontal disease, overweight, obesity and diabetes [8]. However, many commercial  $\alpha$ -amylase  
60 inhibitors have complained of intestinal side effects [4]. In order to avoid the unwanted side effects  
61 of current drugs, many efforts are devoted to the discovery of new inhibitors of carbohydrate  
62 digestion.

63 Flavonoids are secondary metabolites constituting the largest group of natural polyphenols. They  
64 are commonly found in plants and responsible for the attractive colors of flowers and fruits [9]. The  
65 flavonoid structure has a C<sub>15</sub> carbon skeleton consisting of two aromatic rings (A) and (B) linked  
66 together by a C<sub>3</sub> chain forming the heterocycle (C) [10]. Moreover, 2-phenylbenzopyrane  
67 flavonoids were classified into many categories, distinguished by cyclization, degree of  
68 unsaturation and oxidation and by the pyranic cycle (C) substitution [10-11]. On the other hand,  
69 numerous flavonoid compounds, such as rutin, quercetagenin, scutellarein, 8-prenylapigenin, fisetin,  
70 luteolin and quercetin (Figure 1), were reported as antidiabetics [12-17] and  $\alpha$ -amylase inhibitors  
71 [5,18-19], together with different other biological properties [20-27]. However, the broad biological  
72 profile of flavonoids has encouraged chemical researchers to synthesize these remarkable  
73 compounds with special chemical substituents and targeted bioactivities [28-32].

74 **Fig. 1.** Example of flavonoids previously reported as antidiabetics.

75

76 Moreover, in a previous study, it was shown that the presence of bromine atom was found to be  
77 essential in the structure of the most inhibitory derivatives of the  $\alpha$ -amylase enzyme [33], thus  
78 dictating their presence as one of the main parts of the structure of future  $\alpha$ -amylase inhibitors. On  
79 the other hand, the metabolic stability, the strong electron withdrawing character and the lipophilic  
80 nature of the trifluoromethyl moiety allow an increase in their demand for the development of  
81 bioactive compounds [34]. Otherwise, lipophilicity, an important physicochemical property of  
82 bioactive compounds, has a molecule penetration role through the cell membrane [35], thus  
83 increasing the binding to receptor pockets, which supposes a powerful activity. Hence, many  
84 important drugs are trifluoromethylated compounds, viz. fluphenazine (antipsychotic, anticancer)  
85 [36], leflunomide (antirheumatic) [37], celecoxib (COX-2 selective inhibitor) [38], fluoxetine  
86 (antidepressant) [39], and fluazinam (fungicide) [40] (Figure 2). In addition, a trifluoromethylated  
87 5-amino-nicotinic acid derivative has been reported to exhibit promising  $\alpha$ -amylase and  $\alpha$ -  
88 glucosidase inhibitors [41].

89  
90 **Fig. 2.** Structures of trifluoromethylated drugs.

91  
92 Furthermore, isoxazole (1,2-oxazole) is a five-membered aromatic monocyclic heteroarene. It is of  
93 a great importance in medicinal chemistry. In addition, natural products containing isoxazole ring,  
94 such as ibotenic acid (neurotoxin and hallucinogenic) and muscimol (hallucinogenic and GABA<sub>A</sub>  
95 receptor antagonist) (Figure 3a) [42-45], have aroused the interest from pharmacologists and  
96 chemists because of their potent biological and pharmacological properties. Therefore, the isoxazole  
97 heterocycle has been extensively used as a key building block for drugs such as valdecoxib,  
98 parecoxib (COX-2 inhibitors) [46], zonisamide (anti-convulsant) [47] and leflunomide  
99 (antirheumatic) [37]. Furthermore, 1,2-oxazole derivatives are reported to possess a wide spectrum

100 of biological properties such as antidiabetics (Figure 3b) [48], along with other bioactivities viz.  
101 analgesic, anti-inflammatory, anti-HIV, and anti-cancer [49-53].

102

103 **Fig. 3. (a)** Natural compounds containing isoxazole ring. **(b)** Previously reported isoxazole  
104 derivatives as antidiabetic agents. **(c)** Reported flavonoid-based isoxazoles with antidiabetic  
105 properties.

106

107 To the best of our knowledge, there is only one previous study reported that flavonoid-based  
108 isoxazoles exhibit antidiabetic properties, which have improved the glucose consumption in insulin  
109 resistant HepG2 cells. Also, it turned out to be important to indicate that the studied structures were  
110 limited to the 3-(4-cyanophenyl)isoxazole derivatives (Figure 3c) [54].

111 According to the potential  $\alpha$ -amylase inhibition and antidiabetic activities of flavonoids and  
112 isoxazole derivatives and the inspiration from the findings cited above, the present work was  
113 performed to discover new hybrid molecules, where a halogenated flavonoid was joined to a 3-  
114 arylisoxazole moiety *via* a methylene linker in order to increase the  $\alpha$ -amylase inhibitory potency.  
115 Hence, the structure-activity relationship was *in silico* approved by the molecular docking analysis.  
116 In addition, the characterization of the structural and the vibrational spectroscopic properties of the  
117 synthesized molecules were performed using DFT methods at the B3LYP/6-311++G (d,p) level of  
118 theory. The physicochemical properties of these compounds were evaluated using the software  
119 HyperChem 8.03, and from which various physicochemical and quantum descriptor parameters  
120 were deduced.

121

## 122 **2. Material and methods**

### 123 *2.1. General experimental procedures*

124 <sup>1</sup>H NMR (300 MHz), DEPT 135 and <sup>13</sup>C NMR (75 MHz) spectra were recorded in deuterated  
125 chloroform and dimethyl sulfoxide-*d*<sub>6</sub> with a Bruker AC-300 spectrometer. All chemical shifts (δ)  
126 were reported in parts per million (ppm), coupling constants (*J*) were given in Hertz (Hz) and  
127 residual non-deuterated solvent resonance was used as internal reference. DCI-HRMS spectra were  
128 run in a GCT 1er Waters in the positive ion mode. ESI-HRMS were recorded with ESI-TOF (LCT,  
129 Waters) in the positive ion mode using the reflectron mode. All chemical reactions were monitored  
130 by commercial TLC plates (Silica gel 60, F<sub>254</sub>). All used solvents were freshly distilled prior to use.  
131 Büchi 510 apparatus was used to determine melting points.

## 132 2.2. Chemistry

### 133 2.2.1. General procedure for the synthesis of the flavonol (**1**)

134 The preparation of the halogenated flavonol (**1**), previously synthesized in our laboratory was  
135 reported according to the procedure adopted by Znati et al. (2019) [32]. A mixture of 2 mL of 5-  
136 bromo-2-hydroxyacetophenone (16.61 mmol), 2.89 g of 4-(trifluoromethyl)benzaldehyde (16.61  
137 mmol) and 2 g of NaOH (50 mmol) were added to 100 mL of methanol in a round-bottom flask  
138 (500 mL) equipped with a magnetic stirrer. The obtained solution was heated at reflux for 3 hours.  
139 The reaction mixture was cooled to room temperature for 15 min. Afterwards, 100 mL of NaOH  
140 (0.5M), then 6.84 mL of H<sub>2</sub>O<sub>2</sub> (35%) were added and the solution was stirred for 2 hours at room  
141 temperature. The reaction mixture was poured to give a precipitate into ice-water which is then  
142 recovered by filtration to obtain the flavonol (**1**). The halogenated flavonol (**1**) was obtained with a  
143 yield of 87%.

### 144 6-bromo-3-hydroxy-2-(4-(trifluoromethyl)phenyl)-4H-chromen-4-one (**1**)

145 Red solid, yield: 87%, mp: 270°C. DCI-HRMS [M + H]<sup>+</sup> calcd. for (C<sub>16</sub>H<sub>9</sub>BrF<sub>3</sub>O<sub>3</sub>)<sup>+</sup>: 384.9687,  
146 found: 384.9680. <sup>1</sup>H NMR (DMSO-*d*<sub>6</sub>, 300 MHz) δ<sub>H</sub> 8.11 (1H, d, *J* = 2.4 Hz, H-5), 7.71 (1H, dd, *J*<sub>1</sub>  
147 = 9.0, *J*<sub>2</sub> = 2.4 Hz, H-7), 7.64 (1H, d, *J* = 9.0 Hz, H-8), 7.71 (2H, d, *J* = 8.4 Hz, H-2',6'), 8.87 (2H,  
148 d, *J* = 8.4 Hz, H-3',5'). <sup>13</sup>C NMR (DMSO-*d*<sub>6</sub>, 75 MHz) δ<sub>C</sub> 154.9 (C-2), 141.8 (C-3), 179.5 (C-4),

149 127.0 (C-5), 114.5 (C-6), 133.9 (C-7), 121.1 (C-8), 152.7 (C-9), 122.7 (C-10), 139.4 (C-1'), 124.5  
150 (C-2',6'), 124.7 (q,  $^3J_{CF} = 3.6$  Hz, C-3',5'), 125.1 (q,  $^2J_{CF} = 31.0$  Hz, C-4'), 124.9 (q,  $^1J_{CF} = 270.1$  Hz,  
151 C-7').

### 152 2.2.2. General procedure for the synthesis of the dipolarophile (**2**)

153 To a mixture of 3 g of the synthesized flavonol (**1**, 7.81 mmol) in anhydrous DMF, 2 equivalents of  
154  $K_2CO_3$  were added. The solution is kept under stirring for 15 min in an ice bath. Subsequently, 2  
155 equivalents of propargyl bromide are then added. The reaction mixture was stirred for 2 hours at  
156 room temperature and the reaction was monitored by TLC analysis. Once the reaction is complete,  
157 the residue is diluted with 200 mL of distilled water and through sintered glass, the formed  
158 precipitate was then filtered. The dipolarophile **2** was obtained with an excellent yield, 96%.

### 159 6-bromo-3-(prop-2-yn-1-yloxy)-2-(4-(trifluoromethyl)phenyl)-4H-chromen-4-one (**2**)

160 Yellowish solid, yield: 96%, mp: 125°C.  $^1H$  NMR ( $CDCl_3$ , 300 MHz)  $\delta_H$  8.41 (1H, d,  $J = 2.4$  Hz,  
161 H-5), 7.81 (1H, dd,  $J_1 = 8.9$ ,  $J_2 = 2.4$  Hz, H-7), 7.48 (1H, d,  $J = 8.9$  Hz, H-8), 7.81 (2H, d,  $J = 8.2$   
162 Hz, H-2',6'), 8.27 (2H, d,  $J = 8.2$  Hz, H-3',5'), 5.06 (2H, d,  $J = 2.4$  Hz, H-1''), 2.35 (1H, t,  $J = 2.4$   
163 Hz, H-3'').  $^{13}C$  NMR ( $CDCl_3$ , 75 MHz)  $\delta_C$  155.4 (C-2), 139.4 (C-3), 173.8 (C-4), 128.7 (C-5), 118.8  
164 (C-6), 137.1 (C-7), 120.2 (C-8), 154.3 (C-9), 125.5 (C-10), 134.3 (C-1'), 129.5 (C-2',6'), 125.6 (q,  
165  $^3J_{CF} = 3.6$  Hz, C-3',5'), 132.7 (q,  $^2J_{CF} = 32.8$  Hz, C-4'), 123.9 (q,  $^1J_{CF} = 270.7$  Hz, C-7'), 59.6 (C-1''),  
166 78.4 (C-2''), 76.9 (C-3'').

### 167 2.2.3. General procedure for the synthesis of the halogenated flavonoid-based isoxazoles **2a-m**

168 A mixture of 50 mg of the dipolarophile (**2**), 1.5 equivalents of the appropriate hydroximyl chloride,  
169 2 equivalents of the triethylamine and 0.1 equivalent of CuI were dissolved at room temperature in  
170 2 mL of DMF. The solution was subjected for 5 min to a microwave irradiation at 250 W. Then, the  
171 solution was diluted with distilled water and extracted three times with ethyl acetate (30 mL). After  
172 *in vacuo* solvent removing, the resulting residue was purified by silica gel column chromatography,



173 eluted with a mixture of petroleum ether : ethyl acetate (8:2). The desired products **2a-m** were  
174 obtained with good yields ranging from 72 to 94%.

175 2.2.3.1. 6-bromo-3-((3-phenylisoxazol-5-yl)methoxy)-2-(4-(trifluoromethyl)phenyl)-4H-chromen-  
176 4-one (**2a**)

177 Yellowish solid, yield: 90%, mp: 164°C. <sup>1</sup>H NMR (CDCl<sub>3</sub>, 300 MHz) δ<sub>H</sub> 8.43 (1H, d, *J* = 2.3 Hz,  
178 H-5), 7.81 (1H, dd, *J*<sub>1</sub> = 8.9, *J*<sub>2</sub> = 2.3 Hz, H-7), 7.45 (1H, m, H-8), 7.73 (2H, d, *J* = 8.3 Hz, H-2',6'),  
179 8.10 (2H, d, *J* = 8.3 Hz, H-3',5'), 6.44 (1H, s, H-4''), 5.42 (2H, s, H-6''), 7.67 (2H, m, H-2''',6'''), 7.45  
180 (3H, m, H-3''',4''',5'''). <sup>13</sup>C NMR (CDCl<sub>3</sub>, 75 MHz) δ<sub>C</sub> 155.5 (C-2), 139.7 (C-3), 173.7 (C-4), 128.6  
181 (C-5), 118.9 (C-6), 137.3 (C-7), 120.3 (C-8), 154.3 (C-9), 125.6 (C-10), 133.8 (C-1'), 129.4 (C-  
182 2',6'), 125.6 (q, <sup>3</sup>*J*<sub>CF</sub> = 4.0 Hz, C-3',5'), 132.8 (q, <sup>2</sup>*J*<sub>CF</sub> = 32.8 Hz, C-4'), 123.8 (q, <sup>1</sup>*J*<sub>CF</sub> = 270.8 Hz, C-  
183 7'), 167.8 (C-3''), 103.0 (C-4''), 162.5 (C-5''), 63.8 (C-6''), 128.7 (C-1'''), 126.9 (C-2''',6'''), 129.1 (C-  
184 3''',5'''), 130.4 (C-4''').

185 2.2.3.2. 6-bromo-3-((3-(4-fluorophenyl)isoxazol-5-yl)methoxy)-2-(4-(trifluoromethyl)phenyl)-4H-  
186 chromen-4-one (**2b**)

187 Yellowish solid, yield: 94%, mp: 176°C. <sup>1</sup>H NMR (CDCl<sub>3</sub>, 300 MHz) δ<sub>H</sub> 8.43 (1H, d, *J* = 2.3 Hz,  
188 H-5), 7.82 (1H, dd, *J*<sub>1</sub> = 8.9, *J*<sub>2</sub> = 2.3 Hz, H-7), 7.46 (1H, d, *J* = 8.9 Hz, H-8), 7.73 (2H, d, *J* = 8.3  
189 Hz, H-2',6'), 8.11 (2H, d, *J* = 8.3 Hz, H-3',5'), 6.41 (1H, s, H-4''), 5.41 (2H, s, H-6''), 7.66 (2H, dd,  
190 *J*<sub>1</sub> = 8.6, *J*<sub>2</sub> = 5.3 Hz, H-2''',6'''), 7.13 (2H, t, *J* = 8.6 Hz, H-3''',5'''). <sup>13</sup>C NMR (CDCl<sub>3</sub>, 75 MHz) δ<sub>C</sub>  
191 155.5 (C-2), 139.8 (C-3), 173.6 (C-4), 128.6 (C-5), 119.0 (C-6), 137.3 (C-7), 120.3 (C-8), 154.3 (C-  
192 9), 125.6 (C-10), 133.8 (C-1'), 129.4 (C-2',6'), 125.6 (q, <sup>3</sup>*J*<sub>CF</sub> = 3.7 Hz, C-3',5'), 132.8 (q, <sup>2</sup>*J*<sub>CF</sub> = 32.8  
193 Hz, C-4'), 123.8 (q, <sup>1</sup>*J*<sub>CF</sub> = 271.0 Hz, C-7'), 168.0 (C-3''), 102.8 (C-4''), 161.6 (C-5''), 63.8 (C-6''),  
194 124.9 (d, <sup>4</sup>*J*<sub>CF</sub> = 3.5 Hz, C-1'''), 128.9 (d, <sup>3</sup>*J*<sub>CF</sub> = 8.5 Hz, C-2''',6'''), 116.3 (d, <sup>2</sup>*J*<sub>CF</sub> = 21.8 Hz, C-3''',5'''),  
195 164.1 (d, <sup>1</sup>*J*<sub>CF</sub> = 248.7 Hz, C-4''').

196 2.2.3.3. 6-bromo-3-((3-(4-chlorophenyl)isoxazol-5-yl)methoxy)-2-(4-(trifluoromethyl)phenyl)-4H-  
197 chromen-4-one (**2c**)

198 Yellowish solid, yield: 93%, mp: 191°C. <sup>1</sup>H NMR (CDCl<sub>3</sub>, 300 MHz) δ<sub>H</sub> 8.43 (1H, d, *J* = 2.4 Hz,  
199 H-5), 7.82 (1H, dd, *J*<sub>1</sub> = 8.9, *J*<sub>2</sub> = 2.4 Hz, H-7), 7.46 (1H, d, *J* = 8.9 Hz, H-8), 7.73 (2H, d, *J* = 8.3  
200 Hz, H-2',6'), 8.10 (2H, d, *J* = 8.3 Hz, H-3',5'), 6.42 (1H, s, H-4''), 5.41 (2H, s, H-6''), 7.61 (2H, d, *J*  
201 = 8.6 Hz, H-2''',6'''), 7.42 (2H, d, *J* = 8.6 Hz, H-3''',5'''). <sup>13</sup>C NMR (CDCl<sub>3</sub>, 75 MHz) δ<sub>C</sub> 155.5 (C-2),  
202 139.8 (C-3), 173.6 (C-4), 128.6 (C-5), 119.0 (C-6), 137.3 (C-7), 120.3 (C-8), 154.3 (C-9), 125.6 (C-  
203 10), 133.8 (C-1'), 129.4 (C-2',6'), 125.6 (q, <sup>3</sup>*J*<sub>CF</sub> = 3.6 Hz, C-3',5'), 132.8 (q, <sup>2</sup>*J*<sub>CF</sub> = 32.6 Hz, C-4'),  
204 123.8 (q, <sup>1</sup>*J*<sub>CF</sub> = 271.2 Hz, C-7'), 168.2 (C-3''), 102.8 (C-4''), 161.6 (C-5''), 63.8 (C-6''), 127.2 (C-  
205 1'''), 129.4 (C-2''',6'''), 128.2 (C-3''',5'''), 136.5 (C-4''').

206 2.2.3.4. 6-bromo-3-((3-(4-bromophenyl)isoxazol-5-yl)methoxy)-2-(4-(trifluoromethyl)phenyl)-4H-  
207 chromen-4-one (**2d**)

208 Yellowish solid, yield: 91%, mp: 194°C. ESI-HRMS [M + H]<sup>+</sup> calcd. for (C<sub>26</sub>H<sub>15</sub>Br<sub>2</sub>F<sub>3</sub>NO<sub>4</sub>)<sup>+</sup>:  
209 619.9320, found: 619.9296. <sup>1</sup>H NMR (CDCl<sub>3</sub>, 300 MHz) δ<sub>H</sub> 8.43 (1H, d, *J* = 2.4 Hz, H-5), 7.82  
210 (1H, dd, *J*<sub>1</sub> = 8.9, *J*<sub>2</sub> = 2.4 Hz, H-7), 7.46 (1H, d, *J* = 8.9 Hz, H-8), 7.73 (2H, d, *J* = 8.3 Hz, H-2',6'),  
211 8.11 (2H, d, *J* = 8.3 Hz, H-3',5'), 6.43 (1H, s, H-4''), 5.41 (2H, s, H-6''), 7.58 (2H, d, *J* = 8.8 Hz, H-  
212 2''',6'''), 7.54 (2H, d, *J* = 8.8 Hz, H-3''',5'''). <sup>13</sup>C NMR (CDCl<sub>3</sub>, 75 MHz) δ<sub>C</sub> 155.4 (C-2), 139.8 (C-3),  
213 173.6 (C-4), 128.6 (C-5), 119.0 (C-6), 137.3 (C-7), 120.3 (C-8), 154.3 (C-9), 125.6 (C-10), 133.8  
214 (C-1'), 129.4 (C-2',6'), 125.6 (q, <sup>3</sup>*J*<sub>CF</sub> = 3.4 Hz, C-3',5'), 132.9 (q, <sup>2</sup>*J*<sub>CF</sub> = 32.6 Hz, C-4'), 123.8 (q,  
215 <sup>1</sup>*J*<sub>CF</sub> = 271.5 Hz, C-7'), 168.2 (C-3''), 102.7 (C-4''), 161.7 (C-5''), 63.8 (C-6''), 127.7 (C-1'''), 128.4  
216 (C-2''',6'''), 132.4 (C-3''',5'''), 124.7 (C-4''').

217 2.2.3.5. 6-bromo-3-((3-(*p*-tolyl)isoxazol-5-yl)methoxy)-2-(4-(trifluoromethyl)phenyl)-4H-chromen-  
218 4-one (**2e**)

219 Yellowish solid, yield: 90%, mp: 172°C. <sup>1</sup>H NMR (CDCl<sub>3</sub>, 300 MHz) δ<sub>H</sub> 8.43 (1H, d, *J* = 2.4 Hz,  
220 H-5), 7.81 (1H, dd, *J*<sub>1</sub> = 8.9, *J*<sub>2</sub> = 2.4 Hz, H-7), 7.45 (1H, d, *J* = 8.9 Hz, H-8), 7.73 (2H, d, *J* = 8.3  
221 Hz, H-2',6'), 8.10 (2H, d, *J* = 8.3 Hz, H-3',5'), 6.41 (1H, s, H-4''), 5.41 (2H, s, H-6''), 7.56 (2H, d, *J*  
222 = 8.0 Hz, H-2''',6'''), 7.24 (2H, d, *J* = 8.0 Hz, H-3''',5'''), 2.40 (3H, s, H-7'''). <sup>13</sup>C NMR (CDCl<sub>3</sub>, 75

223 MHz)  $\delta_C$  155.5 (C-2), 139.7 (C-3), 173.7 (C-4), 128.6 (C-5), 118.9 (C-6), 137.2 (C-7), 120.3 (C-8),  
224 154.3 (C-9), 125.6 (C-10), 133.8 (C-1'), 129.4 (C-2',6'), 125.6 (q,  $^3J_{CF} = 3.7$  Hz, C-3',5'), 132.8 (q,  
225  $^2J_{CF} = 32.7$  Hz, C-4'), 123.8 (q,  $^1J_{CF} = 270.5$  Hz, C-7'), 167.6 (C-3''), 102.9 (C-4''), 162.5 (C-5''),  
226 63.8 (C-6''), 125.9 (C-1'''), 126.8 (C-2''',6'''), 129.8 (C-3''',5'''), 140.5 (C-4'''), 21.6 (C-7''').

227 2.2.3.6. *6-bromo-3-((3-(4-(tert-butyl)phenyl)isoxazol-5-yl)methoxy)-2-(4-(trifluoromethyl)phenyl)-*  
228 *4H-chromen-4-one (2f)*

229 Yellowish solid, yield: 90%, mp: 118°C.  $^1H$  NMR (CDCl<sub>3</sub>, 300 MHz)  $\delta_H$  8.44 (1H, d,  $J = 2.4$  Hz,  
230 H-5), 7.82 (1H, dd,  $J_1 = 8.9$ ,  $J_2 = 2.4$  Hz, H-7), 7.46 (1H, d,  $J = 8.9$  Hz, H-8), 7.73 (2H, d,  $J = 8.3$   
231 Hz, H-2',6'), 8.10 (2H, d,  $J = 8.3$  Hz, H-3',5'), 6.42 (1H, s, H-4''), 5.43 (2H, s, H-6''), 7.61 (2H, d,  $J$   
232 = 8.5 Hz, H-2''',6'''), 7.46 (2H, d,  $J = 8.5$  Hz, H-3''',5'''), 1.36 (9H, s, H-8''').  $^{13}C$  NMR (CDCl<sub>3</sub>, 75  
233 MHz)  $\delta_C$  155.5 (C-2), 139.7 (C-3), 173.7 (C-4), 128.6 (C-5), 118.9 (C-6), 137.2 (C-7), 120.3 (C-8),  
234 154.3 (C-9), 125.6 (C-10), 133.8 (C-1'), 129.4 (C-2',6'), 125.6 (q,  $^3J_{CF} = 3.8$  Hz, C-3',5'), 132.8 (q,  
235  $^2J_{CF} = 32.7$  Hz, C-4'), 123.8 (q,  $^1J_{CF} = 270.8$  Hz, C-7'), 167.5 (C-3''), 103.0 (C-4''), 162.4 (C-5''),  
236 63.8 (C-6''), 125.8 (C-1'''), 126.1 (C-2''',6'''), 126.7 (C-3''',5'''), 153.7 (C-4'''), 35.0 (C-7'''), 31.4 (C-8''').

237 2.2.3.7. *6-bromo-3-((3-(4-nitrophenyl)isoxazol-5-yl)methoxy)-2-(4-(trifluoromethyl)phenyl)-4H-*  
238 *chromen-4-one (2g)*

239 Yellowish solid, yield: 72%, mp: 177°C.  $^1H$  NMR (CDCl<sub>3</sub>, 300 MHz)  $\delta_H$  8.44 (1H, d,  $J = 2.4$  Hz,  
240 H-5), 7.84 (1H, dd,  $J_1 = 8.9$ ,  $J_2 = 2.4$  Hz, H-7), 7.48 (1H, d,  $J = 8.9$  Hz, H-8), 7.74 (2H, d,  $J = 8.3$   
241 Hz, H-2',6'), 8.12 (2H, d,  $J = 8.3$  Hz, H-3',5'), 6.57 (1H, s, H-4''), 5.43 (2H, s, H-6''), 7.87 (2H, d,  $J$   
242 = 8.9 Hz, H-2''',6'''), 8.31 (2H, d,  $J = 8.9$  Hz, H-3''',5''').  $^{13}C$  NMR (CDCl<sub>3</sub>, 75 MHz)  $\delta_C$  155.5 (C-2),  
243 139.8 (C-3), 173.6 (C-4), 128.7 (C-5), 119.1 (C-6), 137.4 (C-7), 120.3 (C-8), 154.3 (C-9), 125.6 (C-  
244 10), 133.7 (C-1'), 129.4 (C-2',6'), 125.6 (q,  $^3J_{CF} = 3.9$  Hz, C-3',5'), 132.9 (q,  $^2J_{CF} = 32.7$  Hz, C-4'),  
245 124.0 (q,  $^1J_{CF} = 271.0$  Hz, C-7'), 169.0 (C-3''), 102.9 (C-4''), 160.8 (C-5''), 63.8 (C-6''), 134.8 (C-  
246 1'''), 124.4 (C-2''',6'''), 127.8 (C-3''',5'''), 149.1 (C-4''').

247 2.2.3.8. 6-bromo-3-((3-(4-methoxyphenyl)isoxazol-5-yl)methoxy)-2-(4-(trifluoromethyl)phenyl)-  
248 4H-chromen-4-one (**2h**)

249 Yellowish solid, yield: 94%, mp: 152°C. <sup>1</sup>H NMR (CDCl<sub>3</sub>, 300 MHz) δ<sub>H</sub> 8.42 (1H, d, *J* = 2.3 Hz,  
250 H-5), 7.81 (1H, dd, *J*<sub>1</sub> = 8.9, *J*<sub>2</sub> = 2.3 Hz, H-7), 7.45 (1H, d, *J* = 8.9 Hz, H-8), 7.72 (2H, d, *J* = 8.3  
251 Hz, H-2',6'), 8.10 (2H, d, *J* = 8.3 Hz, H-3',5'), 6.38 (1H, s, H-4''), 5.40 (2H, s, H-6''), 7.60 (2H, d, *J*  
252 = 8.7 Hz, H-2''',6'''), 6.95 (2H, d, *J* = 8.7 Hz, H-3''',5'''), 3.86 (3H, s, H-7'''). <sup>13</sup>C NMR (CDCl<sub>3</sub>, 75  
253 MHz) δ<sub>C</sub> 155.4 (C-2), 139.7 (C-3), 173.7 (C-4), 128.6 (C-5), 118.9 (C-6), 137.2 (C-7), 120.3 (C-8),  
254 154.3 (C-9), 125.6 (C-10), 133.8 (C-1'), 129.4 (C-2',6'), 125.6 (q, <sup>3</sup>*J*<sub>CF</sub> = 3.7 Hz, C-3',5'), 132.8 (q,  
255 <sup>2</sup>*J*<sub>CF</sub> = 32.7 Hz, C-4'), 123.8 (q, <sup>1</sup>*J*<sub>CF</sub> = 270.6 Hz, C-7'), 167.5 (C-3''), 102.8 (C-4''), 162.1 (C-5''),  
256 63.8 (C-6''), 121.2 (C-1'''), 128.3 (C-2''',6'''), 114.5 (C-3''',5'''), 161.3 (C-4'''), 55.5 (C-7''').

257 2.2.3.9. 6-bromo-3-((3-(4-butoxyphenyl)isoxazol-5-yl)methoxy)-2-(4-(trifluoromethyl)phenyl)-4H-  
258 chromen-4-one (**2i**)

259 Yellowish solid, yield: 93%, mp: 126°C. <sup>1</sup>H NMR (CDCl<sub>3</sub>, 300 MHz) δ<sub>H</sub> 8.43 (1H, d, *J* = 2.4 Hz,  
260 H-5), 7.81 (1H, dd, *J*<sub>1</sub> = 8.9, *J*<sub>2</sub> = 2.4 Hz, H-7), 7.45 (1H, d, *J* = 8.9 Hz, H-8), 7.73 (2H, d, *J* = 8.3  
261 Hz, H-2',6'), 8.10 (2H, d, *J* = 8.3 Hz, H-3',5'), 6.37 (1H, s, H-4''), 5.40 (2H, s, H-6''), 7.58 (2H, d, *J*  
262 = 8.8 Hz, H-2''',6'''), 6.94 (2H, d, *J* = 8.8 Hz, H-3''',5'''), 4.01 (2H, t, *J* = 6.5 Hz, H-7'''), 1.80 (2H, m,  
263 H-8'''), 1.52 (2H, m, H-9'''), 1.00 (3H, t, *J* = 7.3 Hz, H-10'''). <sup>13</sup>C NMR (CDCl<sub>3</sub>, 75 MHz) δ<sub>C</sub> 155.5  
264 (C-2), 139.7 (C-3), 173.7 (C-4), 128.6 (C-5), 118.9 (C-6), 137.2 (C-7), 120.3 (C-8), 154.2 (C-9),  
265 125.5 (C-10), 133.7 (C-1'), 129.4 (C-2',6'), 125.5 (q, <sup>3</sup>*J*<sub>CF</sub> = 3.6 Hz, C-3',5'), 132.7 (q, <sup>2</sup>*J*<sub>CF</sub> = 32.6  
266 Hz, C-4'), 123.8 (q, <sup>1</sup>*J*<sub>CF</sub> = 270.9 Hz, C-7'), 167.3 (C-3''), 102.8 (C-4''), 162.1 (C-5''), 63.7 (C-6''),  
267 120.8 (C-1'''), 128.2 (C-2''',6'''), 115.0 (C-3''',5'''), 160.9 (C-4'''), 68.0 (C-7'''), 31.4 (C-8'''), 19.4 (C-9'''),  
268 14.0 (C-10''').

269 2.2.3.10. 6-bromo-3-((3-(4-butoxy-3-chlorophenyl)isoxazol-5-yl)methoxy)-2-(4-  
270 (trifluoromethyl)phenyl)-4H-chromen-4-one (**2j**)

271 Yellowish solid, yield: 91%, mp: 140°C. ESI-HRMS [M + H]<sup>+</sup> calcd. for (C<sub>30</sub>H<sub>23</sub>BrClF<sub>3</sub>NO<sub>5</sub>)<sup>+</sup>:  
272 648.0400, found: 648.0397. <sup>1</sup>H NMR (CDCl<sub>3</sub>, 300 MHz) δ<sub>H</sub> 8.42 (1H, d, *J* = 2.4 Hz, H-5), 7.81  
273 (1H, dd, *J*<sub>1</sub> = 8.9, *J*<sub>2</sub> = 2.4 Hz, H-7), 7.45 (1H, d, *J* = 8.9 Hz, H-8), 7.73 (2H, d, *J* = 8.3 Hz, H-2',6'),  
274 8.10 (2H, d, *J* = 8.3 Hz, H-3',5'), 6.38 (1H, s, H-4''), 5.39 (2H, s, H-6''), 7.69 (1H, d, *J* = 2.1 Hz, H-  
275 2'''), 6.95 (1H, d, *J* = 8.6 Hz, H-5'''), 7.50 (1H, dd, *J*<sub>1</sub> = 8.6, *J*<sub>2</sub> = 2.1 Hz, H-6'''), 4.08 (2H, t, *J* = 6.5  
276 Hz, H-7'''), 1.86 (2H, m, H-8'''), 1.56 (2H, m, H-9'''), 1.01 (3H, t, *J* = 7.4 Hz, H-10'''). <sup>13</sup>C NMR  
277 (CDCl<sub>3</sub>, 75 MHz) δ<sub>C</sub> 155.4 (C-2), 139.7 (C-3), 173.6 (C-4), 128.6 (C-5), 118.9 (C-6), 137.3 (C-7),  
278 120.3 (C-8), 154.3 (C-9), 125.6 (C-10), 133.8 (C-1'), 129.4 (C-2',6'), 125.6 (q, <sup>3</sup>*J*<sub>CF</sub> = 3.6 Hz, C-  
279 3',5'), 132.8 (q, <sup>2</sup>*J*<sub>CF</sub> = 32.6 Hz, C-4'), 123.8 (q, <sup>1</sup>*J*<sub>CF</sub> = 269.9 Hz, C-7'), 167.8 (C-3''), 102.6 (C-4''),  
280 161.3 (C-5''), 63.8 (C-6''), 121.7 (C-1'''), 128.7 (C-2'''), 123.8 (C-3'''), 156.3 (C-4'''), 113.4 (C-5'''),  
281 126.4 (C-6'''), 69.2 (C-7'''), 31.3 (C-8'''), 19.4 (C-9'''), 14.0 (C-10''').

282 2.2.3.11. 6-bromo-3-((3-(3-chloro-4-methoxyphenyl)isoxazol-5-yl)methoxy)-2-(4-

283 (trifluoromethyl)phenyl)-4H-chromen-4-one (**2k**)

284 Yellowish solid, yield: 90%, mp: 141°C. ESI-HRMS [M + H]<sup>+</sup> calcd. for (C<sub>27</sub>H<sub>17</sub>BrClF<sub>3</sub>NO<sub>5</sub>)<sup>+</sup>:  
285 605.9931, found: 605.9924. <sup>1</sup>H NMR (CDCl<sub>3</sub>, 300 MHz) δ<sub>H</sub> 8.43 (1H, d, *J* = 2.4 Hz, H-5), 7.82  
286 (1H, dd, *J*<sub>1</sub> = 8.9, *J*<sub>2</sub> = 2.4 Hz, H-7), 7.46 (1H, d, *J* = 8.9 Hz, H-8), 7.73 (2H, m, H-2',6'), 8.11 (2H,  
287 d, *J* = 8.2 Hz, H-3',5'), 6.39 (1H, s, H-4''), 5.40 (2H, s, H-6''), 7.71 (1H, m, H-2'''), 6.97 (1H, d, *J* =  
288 8.5 Hz, H-5'''), 7.54 (1H, dd, *J*<sub>1</sub> = 8.5, *J*<sub>2</sub> = 1.9 Hz, H-6'''), 3.96 (3H, s, H-7'''). <sup>13</sup>C NMR (CDCl<sub>3</sub>, 75  
289 MHz) δ<sub>C</sub> 155.4 (C-2), 139.7 (C-3), 173.6 (C-4), 128.5 (C-5), 118.9 (C-6), 137.3 (C-7), 120.3 (C-8),  
290 154.2 (C-9), 125.5 (C-10), 133.7 (C-1'), 129.4 (C-2',6'), 125.5 (q, <sup>3</sup>*J*<sub>CF</sub> = 3.2 Hz, C-3',5'), 132.7 (q,  
291 <sup>2</sup>*J*<sub>CF</sub> = 32.7 Hz, C-4'), 123.8 (q, <sup>1</sup>*J*<sub>CF</sub> = 269.7 Hz, C-7'), 167.8 (C-3''), 102.6 (C-4''), 161.1 (C-5''),  
292 63.7 (C-6''), 122.0 (C-1'''), 128.7 (C-2'''), 123.3 (C-3'''), 156.6 (C-4'''), 112.2 (C-5'''), 126.5 (C-6'''),  
293 56.4 (C-7''').

294 2.2.3.12. 6-bromo-3-((3-(3-bromo-4-methoxyphenyl)isoxazol-5-yl)methoxy)-2-(4-

295 (trifluoromethyl)phenyl)-4H-chromen-4-one (**2l**)

296 Yellowish solid, yield: 89%, mp: 164°C. ESI-HRMS  $[M + H]^+$  calcd. for  $(C_{27}H_{17}Br_2F_3NO_5)^+$ :  
297 649.9426, found: 649.9409.  $^1H$  NMR ( $CDCl_3$ , 300 MHz)  $\delta_H$  8.43 (1H, d,  $J = 2.4$  Hz, H-5), 7.82  
298 (1H, dd,  $J_1 = 8.9$ ,  $J_2 = 2.4$  Hz, H-7), 7.46 (1H, d,  $J = 8.9$  Hz, H-8), 7.73 (2H, d,  $J = 8.3$  Hz, H-2',6'),  
299 8.11 (2H, d,  $J = 8.3$  Hz, H-3',5'), 6.40 (1H, s, H-4''), 5.40 (2H, s, H-6''), 7.88 (1H, d,  $J = 2.0$  Hz, H-  
300 2'''), 6.94 (1H, d,  $J = 8.5$  Hz, H-5'''), 7.59 (1H, dd,  $J_1 = 8.5$ ,  $J_2 = 2.0$  Hz, H-6'''), 3.95 (3H, s, H-7''').  
301  $^{13}C$  NMR ( $CDCl_3$ , 75 MHz)  $\delta_C$  155.5 (C-2), 139.7 (C-3), 173.6 (C-4), 128.6 (C-5), 119.0 (C-6),  
302 137.3 (C-7), 120.3 (C-8), 154.3 (C-9), 125.6 (C-10), 133.8 (C-1'), 129.4 (C-2',6'), 125.6 (q,  $^3J_{CF} =$   
303 3.7 Hz, C-3',5'), 132.8 (q,  $^2J_{CF} = 33.0$  Hz, C-4'), 123.8 (q,  $^1J_{CF} = 270.8$  Hz, C-7'), 167.9 (C-3''),  
304 102.7 (C-4''), 161.1 (C-5''), 63.8 (C-6''), 122.5 (C-1'''), 131.9 (C-2'''), 112.5 (C-3'''), 157.6 (C-4'''),  
305 112.2 (C-5'''), 127.3 (C-6'''), 56.6 (C-7''').

306 2.2.3.13. 6-bromo-3-((3-(3,4-dimethoxyphenyl)isoxazol-5-yl)methoxy)-2-(4-  
307 (trifluoromethyl)phenyl)-4H-chromen-4-one (**2m**)

308 Yellowish solid, yield: 90%, mp: 148°C. ESI-HRMS  $[M + H]^+$  calcd. for  $(C_{28}H_{20}BrF_3NO_6)^+$ :  
309 602.0426, found: 602.0423.  $^1H$  NMR ( $CDCl_3$ , 300 MHz)  $\delta_H$  8.41 (1H, d,  $J = 2.4$  Hz, H-5), 7.80  
310 (1H, dd,  $J_1 = 8.9$ ,  $J_2 = 2.4$  Hz, H-7), 7.45 (1H, d,  $J = 8.9$  Hz, H-8), 7.73 (2H, d,  $J = 8.3$  Hz, H-2',6'),  
311 8.11 (2H, d,  $J = 8.3$  Hz, H-3',5'), 6.41 (1H, s, H-4''), 5.40 (2H, s, H-6''), 7.31 (1H, d,  $J = 1.9$  Hz, H-  
312 2'''), 6.89 (1H, d,  $J = 8.3$  Hz, H-5'''), 7.13 (1H, dd,  $J_1 = 8.3$ ,  $J_2 = 1.9$  Hz, H-6'''), 3.93 (6H, s, H-7''',8''').  
313  $^{13}C$  NMR ( $CDCl_3$ , 75 MHz)  $\delta_C$  155.4 (C-2), 139.7 (C-3), 173.6 (C-4), 128.6 (C-5), 118.9 (C-6),  
314 137.2 (C-7), 120.3 (C-8), 154.2 (C-9), 125.6 (C-10), 133.8 (C-1'), 129.4 (C-2',6'), 125.6 (q,  $^3J_{CF} =$   
315 3.8 Hz, C-3',5'), 132.7 (q,  $^2J_{CF} = 32.7$  Hz, C-4'), 123.8 (q,  $^1J_{CF} = 270.8$  Hz, C-7'), 167.5 (C-3''),  
316 102.8 (C-4''), 162.2 (C-5''), 63.8 (C-6''), 121.4 (C-1'''), 109.4 (C-2'''), 151.0 (C-3'''), 149.6 (C-4'''),  
317 111.3 (C-5'''), 120.1 (C-6'''), 56.2 (C-7'''), 56.2 (C-8''').

### 318 2.3. $\alpha$ -Amylase inhibitory assay

319 The inhibition of  $\alpha$ -amylase enzyme assays was performed according to the protocol described by  
320 Chortani et al. (2021) [55]. Each compound was dissolved in the minimum of DMSO at different

321 concentrations and then diluted in sodium phosphate buffer (0.02 M, pH 6.9 with 0.006 M NaCl).  
322 The DMSO level does not exceed 1% in the mixture. After that, 50  $\mu$ L of each sample solution was  
323 added to 50  $\mu$ L of  $\alpha$ -amylase solution (0.5 mg/mL dissolved in the same buffer medium. After pre-  
324 incubation for 10 min at 25°C, 50  $\mu$ L of the starch solution (1% in buffer solution) was added to the  
325 mixture. After incubation at 25°C for 10 min, the reaction was mixed with 100  $\mu$ L of 3,5-  
326 dinitrosalicylic acid (DNS) solution. At this point, the test tubes were placed in a boiling water bath  
327 for 5 min, followed by cooling to room temperature. Next, each solution was diluted with 1 mL of  
328 distilled water. Over time, the absorbance was measured at 540 nm by Thermo Scientific™  
329 Multiskan™ GO Microplate Spectrophotometer using a 96-well microplate.

330 The  $\alpha$ -amylase inhibitory activity was determined as follows:

$$331 \quad \text{Inhibition (\%)} = 100[(\text{Abs}_{\text{Control}} - \text{Abs}_{\text{Sample}})/(\text{Abs}_{\text{Control}})]$$

332 Where  $\text{Abs}_{\text{Control}}$  is the absorbance of the solution without sample (buffer instead of the sample  
333 solution) and  $\text{Abs}_{\text{Sample}}$  is the absorbance of the mixture with the solution of the sample to be tested.  
334 The concentration of the compound providing 50% inhibition ( $\text{IC}_{50}$ ) was calculated by plotting  
335 inhibition percentages against sample concentrations. Acarbose was used as a positive control. Each  
336 assay was conducted in triplicate.

#### 337 2.4. Molecular Docking procedure

338 The chemical structures of acarbose and the synthesized compounds (**1**, **2** and **2a-m**) were  
339 generated, optimized and their energies were minimized using ACD (3D viewer) software [56]. The  
340 crystal structure of *Aspergillus oryzae*  $\alpha$ -amylase protein (PDB: 7TAA) was downloaded from the  
341 RCSB data bank [57]. The protein was prepared by removing water molecules and the complexed  
342 inhibitor ligand. Then, the polar hydrogens were added followed by appending Kollman charges.  
343 Hence, the grid box, with dimensions of 65 x 52 x 52 points, spacing of 0.375 Å and centered with  
344 coordinates x: 38.725, y: 44.127, and z: 25.633, was generated based on acarbose binding position  
345 in the target protein binding site. The Molecular Docking analyzes of acarbose and the synthesized

346 compounds (**1**, **2** and **2a-m**) were performed using AutoDock Vina software [58]. Molecule-enzyme  
347 interactions were drawn and construed by employing the Biovia Discovery Studio Visualizer  
348 (BIOVIA, D. S. (2017)).

### 349 2.5. DFT studies

350 The optimization of all geometries was performed by Density Functional Theory (DFT) using the  
351 Gaussian 09 set of programs [59]. Geometry optimization of all molecules was carried out using  
352 DFT methods at the B3LYP/6-311++G (d,p) level of theory [60] with Grimme D3 corrections,  
353 updated to include dispersion correlation [61] parameterized by Becke-Johnson (D3BJ). For these  
354 systems, full geometry optimization in the C1 point group was carried out, followed by harmonic  
355 frequencies simulations to confirm that they correspond to true minima (all positive frequencies).  
356 All the calculations were done in DMF, using conductor like polarizable continuum (CPCM). The  
357 conceptual DFT descriptors [62-64] have been computed using the so-called frozen core  
358 approximation and the Koopmans theorem [65]. In addition, the stability of flavonoid-based  
359 isoxazoles was investigated with natural bond orbital analysis (NBO) [66] using NBO6 to  
360 determine the contribution of different interactions in the stability of these reactive compounds,  
361 precisely compound **2b**, the most bioactive one. This evaluation was done at B3LYP/6-  
362 311++G(d,p) level of theory. Compound **2b**, the most  $\alpha$ -amylase inhibitor, was taken as a reference  
363 in this study.

364 On the other hand, Quantitative Structure-Activity Relationship (QSAR) modeling was used as  
365 implemented in HyperChem 8.03 software [67] to identify the physicochemical properties of  
366 halogenated flavonoid-based isoxazole derivatives. Moreover, different types of descriptors viz.  
367 topological descriptors (polarizability (Pol), molar refractivity (MR), partition coefficient  
368 octanol/water (log P), molar volume (MV), surface area grid (SAG), molar weight (MW),  
369 electronic descriptors (LUMO ( $E_{LUMO}$ ) and HOMO ( $E_{HOMO}$ ) energies), and geometric descriptors  
370 (solvent accessible hardness and potential) were used [68-71].



371 *2.6. Statistical analysis*

372 Statistical analysis was carried out using Graph Pad Prism 7.0 (Graph Pad Software Inc., CA, and  
373 USA). All the data are presented as the mean  $\pm$  standard error of the mean (SEM). The difference  
374 between two groups was evaluated using Student's t-test. Significant difference among three or  
375 more groups was determined by one-way ANOVA with a post hoc analysis.

376

377 **3. Results and discussion**

378 *3.1. Chemistry*

379 The 5-bromo-2-hydroxyacetophenone was condensed with 4-(trifluoromethyl)benzaldehyde in the  
380 presence of NaOH for 3 hours at the reflux of methanol, yielding the 5-bromo-4'-(trifluoromethyl)-  
381 2-hydroxychalcone. Afterwards, the cyclization of the ring C and the oxidation of carbon C-3 are  
382 performed by adding H<sub>2</sub>O<sub>2</sub> and NaOH. The reaction mixture was stirred for 2 hours at room  
383 temperature (Scheme 1). The compound **1** was obtained in 87% yield after precipitation in ice-  
384 water.

385

386 **Scheme 1.** Synthetic pathway of the halogenated flavonol (**1**).

387

388 The structure of flavonol (**1**) was confirmed by spectroscopic analysis and by comparison with  
389 literature data [32].

390 On the other hand, 1,3-dipolar cycloaddition is considered the most important synthetic way of a  
391 wide range of isoxazoles. Furthermore, the regiospecific synthesis of isoxazoles catalyzed by Cu(I)  
392 under microwave irradiation is based on the [3 + 2] cycloaddition between terminal alkynes  
393 (dipolarophiles) and aryl nitrile oxides (dipoles) providing only 3,5-disubstituted regioisomers  
394 [53,72].

395 The approach to target the halogenated flavonoid-based isoxazoles (**2a-m**), firstly started by the  
396 preparation of the dipolarophile **2** via the propargylation of the hydroxyl group in position C-3 of  
397 flavonol **1**, in anhydrous DMF for 2 hours at room temperature, in the presence of K<sub>2</sub>CO<sub>3</sub>, as  
398 illustrated in Scheme 2. The dipolarophile **2** was prepared with an excellent yield (96%).

399

400 **Scheme 2.** Synthetic pathway of dipolarophile (**2**).

401

402 The dipolarophile structure (**2**) was established according to its spectral data. Indeed, in addition to  
403 the signals corresponding to the protons and carbons introduced by the flavonol (**1**), new signals of  
404 the propargyl moiety were observed in the <sup>1</sup>H and <sup>13</sup>C NMR spectra. The <sup>1</sup>H NMR spectrum of **2**  
405 recorded in the CDCl<sub>3</sub> at 300 MHz, showed a doublet at δ<sub>H</sub> 5.06 (2H, d, *J* = 2.4 Hz) attributable to  
406 the methylene protons H-1'' and a triplet at δ<sub>H</sub> 2.35 (1H, t, *J* = 2.4 Hz) attributable to the proton of  
407 the ethynyl group (H-3''). The <sup>13</sup>C NMR spectrum confirmed the introduction of the propargyl  
408 group by the observation of new signals at δ<sub>C</sub> 78.4, 76.9 and 59.6 attributable to C-2'', C-3'' and C-  
409 1'', respectively.

410 The 1,3-dipolar cycloaddition reaction was applied in a regiospecific approach using the terminal  
411 alkyne (**2**) and the different hydroximyl chlorides **a-m** variously substituted. Hydroximyl chlorides  
412 **a-m** are the main precursors for the *in situ* generation of aryl nitrile oxides. All the reactions were  
413 conducted under microwave irradiation (250 W) in DMF in the presence of triethylamine and CuI  
414 for 5 minutes (Scheme 3).

415

416 **Scheme 3.** Synthetic pathway of halogenated flavonoid-based isoxazoles **2a-m**.

417

418 The newly prepared 3,5-disubstituted isoxazoles (**2a-m**) were obtained in good yields ranging from  
419 72 to 94%. Their structures are given in Figure 4.

420

421

**Fig. 4.** Structures of the halogenated flavonoid-based isoxazoles (**2a-m**).

422

423

424

425

426

427

428

429

430

431

432

433

434

435

436

437

438

439

440

441

442

443

444

The structures of the synthesized halogenated flavonoid-based isoxazoles **2a-m** (Figure 4) were determined by means of  $^1\text{H}$ ,  $^{13}\text{C}$  NMR and DEPT 135 spectra. The  $^1\text{H}$  NMR spectra of these compounds showed a singlet resonating at  $\delta_{\text{H}}$  6.30-6.60 attributable to the methine proton H-4'' of the isoxazole ring, a singlet at  $\delta_{\text{H}}$  5.35-5.45 attributable to the methylene protons H-6'' and other signals in the aromatic proton zone relating to the protons introduced by the aryl group. Moreover, these structures were also confirmed by  $^{13}\text{C}$  NMR and DEPT 135 spectra, showing all the expected signals from the carbons, essentially the aromatic carbons introduced by the used hydroximyl chlorides, the carbon of the methine C-4'' in the isoxazole ring resonating at  $\delta_{\text{C}}$  102.5-103.0, and the carbon whose signal is inverted in the DEPT 135 spectrum resonating at  $\delta_{\text{C}}$  63.5-63.9 attributable to the unique methylene C-6''.

### 3.2. Evaluation of $\alpha$ -Amylase inhibition

Inhibition is one of successful therapeutic means for controlling the activity of enzymes. Therefore, inhibiting the enzymatic activity of the  $\alpha$ -amylase is a good way to manage diabetes, obesity and to control overweight, by hindering carbohydrate digestion. In this article, fifteen synthesized compounds (**1**, **2** and **2a-m**) were evaluated for their  $\alpha$ -amylase inhibitory activities. The results were expressed in  $\text{IC}_{50}$  ( $\mu\text{M}$ ) and given in Table 1.

According to the results, the synthesized molecules (**1**, **2** and **2a-m**) possess significant anti- $\alpha$ -amylase activity with  $\text{IC}_{50}$  values ranging from  $16.2 \pm 0.3$  to  $33.3 \pm 0.4$   $\mu\text{M}$ . The cycloadduct **2b** ( $\text{R}_1 = \text{F}$ ,  $\text{R}_2 = \text{H}$ ;  $\text{IC}_{50} = 16.2 \pm 0.3$   $\mu\text{M}$ ) exhibited the highest  $\alpha$ -amylase inhibitory activity, this significant value was found to be comparable to that of the standard substance used (Acarbose,  $\text{IC}_{50} = 15.7 \pm 0.2$   $\mu\text{M}$ ). The compounds **2h**, **2i**, **2k** and **2m** displayed considerable  $\alpha$ -amylase inhibitory effects with  $\text{IC}_{50}$  values ranging from  $17.3 \pm 0.1$  to  $19.3 \pm 0.4$   $\mu\text{M}$ . The rest of compounds

445 were found to be slightly less active against the  $\alpha$ -amylase enzyme ( $IC_{50} = 20.8 \pm 0.2 - 33.3 \pm 0.4$   
446  $\mu\text{M}$ ). The inhibitory  $\alpha$ -amylase activity carried out by the newly synthesized compounds is  
447 consistent with previous reports. Nie et al. (2020) [54] reported that flavonoid isoxazole compounds  
448 could display valuable scaffolds for the discovery of antidiabetic drugs.

449 Furthermore, the halogenated compounds in *para* position of the phenyl group attached to the  
450 isoxazole ring (**2b**, **2c** and **2d**) performed significant inhibitions of  $\alpha$ -amylase enzyme, with  $IC_{50}$   
451 values ranging from  $16.2 \pm 0.3$  to  $21.2 \pm 0.2 \mu\text{M}$ . This finding is in good agreement with the  
452 literature, showing that the presence of halogen atoms (F, Cl and Br) in the structure was essential  
453 for a potent  $\alpha$ -amylase inhibition [33,41]. In addition, the structure-activity relationship study  
454 allowed to conclude that the more the inductive attractor (-I) and mesomeric donor (+ M) effects  
455 increase, the greater the inhibitory power of  $\alpha$ -amylase (activity of fluorinated derivative **2b** ( $R_1 = \text{F}$ ,  
456  $R_2 = \text{H}$ ;  $IC_{50} = 16.2 \pm 0.3 \mu\text{M}$ ) is higher than that of the chlorinated one **2c** ( $R_1 = \text{Cl}$ ,  $R_2 = \text{H}$ ;  $IC_{50} =$   
457  $20.8 \pm 0.2 \mu\text{M}$ ), followed by the brominated one **2d** ( $R_1 = \text{Br}$ ,  $R_2 = \text{H}$ ;  $IC_{50} = 21.2 \pm 0.2 \mu\text{M}$ )). These  
458 findings were found to be consistent with literature data indicating that the  $\alpha$ -amylase inhibition  
459 increases with inductive attractor (-I) and mesomeric donor (+M) effects of halogen atoms [6,41].

460 On the other hand, compound **2h** ( $R_1 = \text{OMe}$ ,  $R_2 = \text{H}$ ;  $IC_{50} = 19.3 \pm 0.4 \mu\text{M}$ ), bearing a *para*-methoxy  
461 group, exhibited an interesting  $\alpha$ -amylase inhibitory activity. This finding is in agreement with  
462 previous results [41]. Moreover, compound **2i** ( $R_1 = \text{O-}n\text{-Bu}$ ,  $R_2 = \text{H}$ ;  $IC_{50} = 17.3 \pm 0.1 \mu\text{M}$ ), bearing  
463 a *para*-substituted butoxy group, perceived higher activity than that of *para*-methoxylated one (**2h**).  
464 The electronic effects of alkoxy groups (-I and +M) comparable to those of halogens, may explain  
465 their significant activities. Besides, the methoxylation or the halogenation in the *meta* position of  
466 the *para*-alkoxylated compounds (**2h** and **2i**), to give the compounds **2j-m** ( $IC_{50} = 17.6 \pm 0.3 - 30.9$   
467  $\pm 0.5 \mu\text{M}$ ), did not show a well-defined effect, they reduced the enzyme activity of the  $\alpha$ -amylase in  
468 some cases and increased it in others, but **2i** remains the most active alkoxyated derivative.

469 Likewise, the compound **2g** ( $R_1 = \text{NO}_2$ ,  $R_2 = \text{H}$ ;  $\text{IC}_{50} = 24.7 \pm 0.3 \mu\text{M}$ ), bearing a *para*-nitro group,  
470 revealed a moderate activity, in agreement with the report of Nawaz et al. (2020) [41]. On the other  
471 hand, unsubstituted (**2a**:  $R_1 = \text{H}$ ,  $R_2 = \text{H}$ ;  $\text{IC}_{50} = 33.2 \pm 0.8 \mu\text{M}$ ), *para*-methylated (**2e**:  $R_1 = \text{CH}_3$ ,  $R_2 =$   
472  $\text{H}$ ;  $\text{IC}_{50} = 32.8 \pm 1.0 \mu\text{M}$ ) and *para-tert*-butylated (**2f**:  $R_1 = \text{tert-Bu}$ ,  $R_2 = \text{H}$ ;  $\text{IC}_{50} = 33.3 \pm 0.4 \mu\text{M}$ )  
473 compounds did not offer remarkable activities compared to their aforementioned analogues. This  
474 finding shows that the increase in the donor inductive effect (+I) does not have practically an effect  
475 on the  $\alpha$ -amylase activity. This result is consistent with the reports of Nawaz et al. (2020) and  
476 Kanwal et al. (2021) [6,41].

477

#### 478 **Table 1**

479  $\alpha$ -Amylase inhibition ( $\text{IC}_{50} \mu\text{M}$ ), binding energy (kcal/mol) and interaction detail of compounds **1**, **2** and  
480 **2a-m** docked in the ABC pocket (PDB: 7TAA).

481

#### 482 *3.3. Molecular Docking Studies*

483 The *in silico* experiments can show the ability of molecules to fit well into the active pocket of the  
484 target enzymes. The binding to several residues, especially with the key residues, can explain the  
485 experimental activities of the tested compounds [73-77].

486  $\alpha$ -Amylase enzyme (EC 3.2.1.1), a glycosylhydrolase, hydrolyzes  $\alpha$ -1,4-glycosidic bonds in  
487 starches, such as amylose. The crystal structure of  $\alpha$ -amylase enzyme (PDB: 7TAA) is composed of  
488 a chain A with a sequence length of 478 amino acids [78].  $\alpha$ -Amylase is one of the most important  
489 key enzymes responsible for carbohydrate digestion [7]. Thus, blocking  $\alpha$ -amylase enzyme offers a  
490 strategy to controlling diabetes and helping in the management of obesity [4,5]. Extensive  
491 molecular docking analysis was executed to explore the binding mode, determine the likely  
492 interactions of synthesized molecules (**1**, **2** and **2a-m**) within the hydrophobic binding pocket of  
493 ABC (Modified acarbose hexasaccharide) of the protein crystal structure of *Aspergillus oryzae*  $\alpha$ -

494 amylase enzyme (PDB: 7TAA) [78] using AutoDock Vina software and rationalize the observed *in*  
495 *vitro*  $\alpha$ -amylase inhibitory activities of the newly synthesized compounds.

496 All the synthesized molecules (**1**, **2** and **2a-m**) and acarbose, used as a standard substance, were *in*  
497 *silico* studied. Binding energies and interaction details (Number of interactions, number of  
498 interacting amino acids, interacting amino acids and hydrogen bonds) of ligands with target enzyme  
499 are presented in Table 1.

500 From the *in silico* docking results (Table 1), it was observed that compounds **1** and **2** exhibited good  
501 binding energies (-7.5 and -7.6 kcal/mol, respectively), within the binding site of the  $\alpha$ -amylase  
502 enzyme (PDB: 7TAA). These values are comparable to that of the standard substance (Acarbose, -  
503 7.9 kcal/mol), which will allow them to fit favorably into the active site of the target enzyme.  
504 Interestingly, the newly synthesized halogenated flavonoid-based isoxazoles (**2a-m**) gave the  
505 expected results. They are properly in the bonding pose and exhibited magnificent binding energies  
506 ranging from -9.6 to -8.0 kcal/mol (Table 1). This would allow everyone to fit favorably into the  
507 active site of the  $\alpha$ -amylase enzyme, better than acarbose.

508 The binding poses of acarbose and the four potent  $\alpha$ -amylase inhibitor compounds (**2b**, **2i**, **2k** and  
509 **2m**) in the target enzyme are shown in Figure 5.

510

511 **Fig. 5.** The binding pose of acarbose, **2b**, **2i**, **2k** and **2m** in  $\alpha$ -amylase enzyme.

512

513 Furthermore, the binding mode of acarbose and the four most active compounds (**2b**, **2i**, **2k** and  
514 **2m**) with  $\alpha$ -amylase enzyme are discussed in the following.

515 Acarbose, the compound used as a standard inhibitor substance of  $\alpha$ -amylase enzyme, exhibited a  
516 good binding energy of -7.9 kcal / mol. Its mode of binding shows that it is involved in twelve non-  
517 covalent interactions with nine amino acids (Table 1). Perfectly, it formed nine conventional  
518 hydrogen bonds with the residues GLN-35, HIS-80, TRP-83, ASP-206, LYS-209, GLU-230, LEU-

519 232, ASP-297 and ASP-340. In addition, three carbon hydrogen bonds have been implicated with  
520 LYS-209 and ASP-340 (Figure 6).

521

522 **Fig. 6.** Acarbose and compound **2b**, **2i**, **2k** et **2m** fits into the hydrophobic binding pocket of ABC  
523 in PDB: 7TAA.

524

525 Compound **2b**, the most potent *in vitro* inhibitor of  $\alpha$ -amylase enzyme in the tested series of  
526 halogenated flavonoid-based isoxazoles, exhibited an excellent binding energy of -9.6 kcal/mol. Its  
527 binding mode shows that it is implicated in fifteen non-covalent interactions with nine amino acids  
528 (Table 1). Perfectly, the 3-(3-(4-fluorophenyl)isoxazol-5-yl)methoxyl moiety forms three halogen  
529 (Fluorine) bonds with GLU-230 and ASP-206 residues, a Pi-Pi T-shaped bond with TYR-82, a Pi-  
530 cation and conventional hydrogen bonds with ARG-344, and Pi-anion and carbon hydrogen bonds  
531 with ASP-340 residue. Additionally, the trifluoromethyl group linked to the aromatic ring B of the  
532 flavonoid skeleton is involved in two alkyl interactions with LEU-166 and LEU-173. Moreover,  
533 flavonoid skeleton is involved in a conventional hydrogen binding with GLN-35, a Pi-anion bond  
534 with ASP-340, and two Pi-Pi Stacked and a Pi-alkyl bonds with TYR-75 (Figure 6).

535 The compound **2i** carried out an attractive binding energy of -9.3 kcal/mol. The binding mode of  
536 this derivative shows that it is involved in seventeen non-covalent interactions with eleven amino  
537 acids (Table 1). Consequently, the 3-(3-(4-butoxyphenyl)isoxazol-5-yl)methoxy group interacts in  
538 the active binding site by a carbon hydrogen bond with GLU-230, an alkyl bond with LEU-232, a  
539 Pi-alkyl binding with HIS-210, a Pi-Pi T-shaped bond with TYR-82, a Pi-cation and two  
540 conventional hydrogen bonds with ARG-344, a carbon hydrogen and a Pi-anion interactions with  
541 ASP-340 residue. Furthermore, the trifluoromethyl moiety is involved in a conventional hydrogen  
542 bond with GLY-167, and two alkyl interactions with LEU-166 and LEU-173. In addition, flavonoid  
543 skeleton is involved in a conventional hydrogen bond with GLN-35, a Pi-anion and a carbon

544 hydrogen bonds with ASP-340, and two Pi-Pi Stacked and a Pi-alkyl bonds with TYR-75 (Figure  
545 6).

546 On the other hand, the compound **2k** exhibited a significant binding energy of -8.8 kcal/mol. Its  
547 binding mode shows that it is implicated in fourteen non-covalent interactions with eleven amino  
548 acids (Table 1). Thoroughly, the 3-(3-(3-chloro-4-methoxyphenyl)isoxazol-5-yl)methoxyl moiety  
549 forms two conventional hydrogen bonds with TYR-83 and HIS-80, two carbon hydrogen bonds  
550 with ASP-206 and ASP-297, two Pi-alkyl interactions with HIS-122 and TYR-82, a Pi-Pi Stacked  
551 binding with TYR-82, and a Pi-cation bond with the ARG-344. Furthermore, the trifluoromethyl  
552 group attached to C-4' of the flavonoid skeleton is involved in two conventional hydrogen bonds  
553 with GLY-167 and TRP-83, and an alkyl bond with the LEU-173. On the other hand, flavonoid  
554 skeleton interacts by a conventional hydrogen binding with GLN-35 and two Pi-Pi Stacked bonds  
555 with TYR-75 (Figure 6).

556 Furthermore, the compound **2m** exhibited an interesting binding energy of -8.7 kcal/mol. Its binding  
557 mode shows that it is involved in fourteen non-covalent interactions with seven amino acids (Table  
558 1). Accordingly, molecular insight of docking analysis suggests that the 3-(3-(3,4-  
559 dimethoxyphenyl)isoxazol-5-yl)methoxyl moiety forms three carbon hydrogen bonds with ASP-  
560 206 and GLU-230 residues, two Pi-sigma and a Pi-alkyl bonds with the LEU-166. Besides, the  
561 trifluoromethyl group is involved in a conventional hydrogen binding with HIS-122, a halogen  
562 (Fluorine) bond with TYR-82, two Pi-alkyl bonds with TYR-82 and HIS-122 and an alkyl  
563 interaction with the LEU-173. In addition, the flavonoid skeleton is involved in a Pi-alkyl and two  
564 Pi-Pi Stacked bonds with the TYR-75 residue (Figure 6).

565 In the *Aspergillus oryzae*  $\alpha$ -amylase enzyme (PDB: 7TAA), the nucleophile and the catalytic  
566 acid/base residues, which are responsible for the cleavage of glycosidic bonds, are ASP-206 and  
567 GLU-230 amino acids, respectively [7]. Therefore, interactions between protein and ligand,  
568 primarily *via* the GLU-230 and ASP-206 residues, are the best way to block the cleavage of



569 glycosidic bonds. In fact, the low binding energy, the correct binding pose, the ability to interact  
570 with key residues of glycosidic cleavage (GLU-230 and ASP-206) and the large number of  
571 interactions in the active pocket of the target enzyme can explain the strong inhibitory  $\alpha$ -amylase  
572 effects establishing by almost compounds.

### 573 3.4. DFT studies

#### 574 3.4.1. Vibrational analysis

575 The anharmonic frequencies, certain characteristic sites of the most active product: 6-bromo-3-((3-  
576 (4-fluorophenyl)isoxazol-5-yl)methoxy)-2-(4-(trifluoromethyl)phenyl)-4*H*-chromen-4-one (**2b**,  
577 IC<sub>50</sub>= 16.2 ± 0.3 μM), are given in Table 2. These data are computed at B3LYP/6311++G (d,p)  
578 levels of theory and using second order perturbation theory (VPT2) approach as implemented in  
579 GAUSSIAN. This flavonoid-based isoxazole derivative is a planar molecule. It belongs to the Cs  
580 point group. It possesses 94 a' and 50 a'' vibrational modes (Table S1). Since there are no  
581 experimental spectra available for this compound, our data can be used for the assignment of these  
582 spectra whenever measured.

583

#### 584 **Table 2**

585 Anharmonic vibrational frequencies (in cm<sup>-1</sup>) of 6-bromo-3-((3-(4-fluorophenyl)isoxazol-5-  
586 yl)methoxy)-2-(4-(trifluoromethyl)phenyl)-4*H*-chromen-4-one as computed using B3LYP in  
587 conjunction with the 6-311++ G (d,p) basis set. Also their assignment was given.

588

#### 589 3.4.2. Characterization of the halogenated flavonoid-based isoxazoles

590 Structures of the thirteen halogenated flavonoid-based isoxazoles **2a-m** are optimized at the  
591 B3LYP/ 6311++G (d,p) level of theory. The optimized structures of newly synthesized molecules  
592 are given in Table S2 of the supplementary material. Close examination of these structures of the  
593 halogenated flavonoid-based isoxasoles shows that the 3-phenylisoxazole moiety within these

594 compounds has a very close structure. Indeed, we compute C=O, C=C, C=N, N-O and O-C  
595 distances of 1.24, 1.43, 1.32, 1.39, 1.37 (all values are given in Å), respectively.

596 Thus, the functionalization of the isoxazole ring slightly disturb its structure. This is confirmed by  
597 the vibrational analysis performed for this series of analogs. Anharmonic frequencies can be  
598 obtained after scaling the corresponding harmonic frequencies by the appropriate scaling factor (by  
599 0.9662 for  $\omega > 1000 \text{ cm}^{-1}$  and by 0.9833 for  $\omega < 1000 \text{ cm}^{-1}$ ) as discussed in previous report [79].

600 Table 3 presents the respective data for C=O, N-O, C=N, and C-O elongations. This table shows  
601 that similar C=N (of  $\sim 1443.7 \text{ cm}^{-1}$ ), C=O (of  $\sim 1604.9 \text{ cm}^{-1}$ ), O-N (of  $\sim 1271.8 \text{ cm}^{-1}$ ), C-O (of  
602  $\sim 1362.3 \text{ cm}^{-1}$ ), elongations values are computed for all compounds. Indeed, they differ by less than  
603  $20 \text{ cm}^{-1}$  within the series. Again, this is due to slight perturbation of the heterocycle upon  
604 functionalization.

605

### 606 **Table 3**

607 Scaled anharmonic vibrational frequencies (in  $\text{cm}^{-1}$ ) (scaling factor 0.9662 [79]) of some elongation  
608 modes of flavonoid-based isoxazole derivatives as computed using B3LYP/6-311++G (d,p).

609

#### 610 *3.4.3. Natural bond orbital (NBO) and molecular electrostatic potential (MESP) surface of* 611 *flavonoid-based isoxazole derivatives (2a-m)*

612 The information contained in molecular electrostatic potentials (MESP) has been harnessed for  
613 determination of structure, reactivity, electron diffraction and scattering and also the energetics of a  
614 wide variety of organic and inorganic, as well as biological molecular systems [80]. In fact, MESP  
615 displays simultaneously the molecular size and shape as well as positive, negative and neutral  
616 electrostatic potential regions in terms of the electrostatic surface [81]. Figure 7 shows the MESP  
617 surface map of the most active compound (**2b**: 6-bromo-3-((3-(4-fluorophenyl)isoxazol-5-  
618 yl)methoxy)-2-(4-(trifluoromethyl)phenyl)-4*H*-chromen-4-one;  $\text{IC}_{50} = 16.2 \pm 0.3 \mu\text{M}$ ). The red color

619 refers to negative potential regions as around the oxygen atom (carbonyl/ C=O) of the pyran ring.  
620 For nitrogen, we compute mostly negative potentials with different magnitudes. These regions are  
621 susceptible for electrophilic attacks. Figure 7 shows also that the regions around the hydrogens  
622 attached to the phenyl ring are blue (positive potentials). These regions are susceptible for  
623 nucleophilic attacks. This analysis agrees with the net charges calculated using natural bond orbital  
624 (NBO) model (Figure 8). The present analyses allow identifying the hydrogen bond donor (HBD)  
625 and hydrogen bond acceptor (HBA) sites (Figure 7). These characteristics may be helpful for a  
626 qualitative understanding of the electrostatic interactions that may take place between reagents or  
627 enzyme active sites and the flavonoid-based isoxazole derivatives (**2a-m**) under study.

628

629 **Fig. 7.** 3D MESP surface map (left) for 6-bromo-3-((3-(4-fluorophenyl)isoxazol-5-yl)methoxy)-2-  
630 (4-(trifluoromethyl)phenyl)-4*H*-chromen-4-one (**2b**) and its hydrogen bond acceptor (HBA) sites  
631 (right). The red regions correspond to negative potentials and the blue regions to positive potentials.

632

633 **Fig. 8.** B3LYP/6-311++G (d,p) net charges calculated using natural bond orbital (NBO) in  
634 compound **2b**.

635

#### 636 3.4.4. *Structural and physicochemical property relationships*

637 The structures of the flavonoid-based isoxazole derivatives are shown in Figure 4. QSAR properties  
638 of compounds **2a-m**, such as octanol-water partition coefficient (logP), molar refractivity (MR),  
639 polarizability (Pol), surface bounded molecular volume, molecular weight (MW), Hardness ( $\eta$ ),  
640 potential ( $\mu$ ), HOMO energy ( $E_{\text{HOMO}}$ , energy of the highest occupied molecular orbital) and LUMO  
641 energy ( $E_{\text{LUMO}}$ , energy of the lowest unoccupied molecular orbital) [82], were listed in Table 4.

642 The polarizability and molar refractivity are connected to the size and the molecular weight of the  
643 halogenated flavonoid-based isoxazoles (**2a-m**). This result is in agreement with the formula of

644 Lorentz-Lorenz [83-84] which provides a relation between polarizability, molar refractivity and  
 645 volume. These findings can be proven by the compound **2a** (6-bromo-3-((3-phenylisoxazol-5-  
 646 yl)methoxy)-2-(4-(trifluoromethyl)phenyl)-4*H*-chromen-4-one, R<sub>1</sub>= H, R<sub>2</sub>= H), the smallest  
 647 molecule of the newly synthesized series, whose molecular weight, polarizability and molar  
 648 refractivity are equal to 542.31 amu, 47.79 Å<sup>3</sup> and 140.54Å<sup>3</sup>, respectively. On the other hand, the  
 649 compound **2j** (6-bromo-3-((3-(4-butoxy-3-chlorophenyl)isoxazol-5-yl)methoxy)-2-(4-  
 650 (trifluoromethyl)phenyl)-4*H*-chromen-4-one, R<sub>1</sub>= O-*n*-Bu, R<sub>2</sub>= Cl) has the highest molecular  
 651 weight (648.86 amu), therefore we note a growth in the polarizability and molar refractivity, 57.69  
 652 Å<sup>3</sup> and 165.50Å<sup>3</sup>, respectively.

653 Several physicochemical descriptors, derived from conceptual DFT, are given in Table 4. They  
 654 describe the reactivity of the studied molecules and can explain the effect of various substituents on  
 655 our core [85], such as chemical potential  $\mu$  ( $\mu = \left(\frac{\partial E}{\partial N}\right)_{v(r)}$ ) and hardness  $\eta$  ( $\eta = \left(\frac{\partial^2 E}{\partial N^2}\right)_{v(r)}$ ) with  
 656  $E_{v(r)}$  is the total energy of the system, N: number of electrons and v(r) indicates that the derivatives  
 657 are taken at constant external potential [86]. These indexes are often approximated through frontier  
 658 orbital eigenvalues, leading to  $\mu \cong (E_{\text{HOMO}} + E_{\text{LUMO}})/2$  and  $\eta \cong (E_{\text{LUMO}} - E_{\text{HOMO}})$  [87].

659 HOMO and LUMO energies are related to the reactivity of the molecule: molecules with electrons  
 660 at accessible (near-zero) HOMO levels tend to be good nucleophiles because it does not cost much  
 661 to donate these electrons toward making a new bond. Similarly, molecules with lower LUMO  
 662 energies tend to be good electrophiles because it does not cost much to place an electron into such  
 663 an orbital. The energy gap which expresses the energy difference between two important FMOs  
 664 (HOMO-LUMO) [88], signifies the chemical hardness-softness, the kinetic stability and the  
 665 reactivity of molecules. Hard molecules with large gap are more stable and less reactive. In the  
 666 opposite case, soft molecules having a gap are more reactive and less stable [89-90]. As can be  
 667 seen, compound **2c** (6-bromo-3-((3-(4-chlorophenyl)isoxazol-5-yl)methoxy)-2-(4-  
 668 (trifluoromethyl)phenyl)-4*H*-chromen-4-one, R<sub>1</sub>= Cl, R<sub>2</sub>= H) has the highest value of LUMO (E = -

669 2.651eV) with energy gap ( $\Delta E = 4.147$  eV), hardness ( $\eta = 2.072$  eV) and potential ( $\mu = -4.725$  eV).  
670 Thus, this compound is the most stable one (Figure 9). Compound **2i** (6-bromo-3-((3-(4-  
671 butoxyphenyl)isoxazol-5-yl)methoxy)-2-(4-(trifluoromethyl)phenyl)-4*H*-chromen-4-one,  $R_1 = O$ -  
672 butyl,  $R_2 = H$ ) has the highest HOMO (-6.224 eV) and the smallest  $\Delta E$  value ( $\Delta E = 3.578$  eV). Thus,  
673 this compound is the most reactive one (Figure 9). Indeed, a group with a negative inductive effect  
674 (-I) like (Cl, F,  $OCH_3$  ...) substituted in para position of the 3-phenylisoxazole core have an  
675 influence on the  $\alpha$ -amylase inhibition activity for instance **2c** ( $IC_{50} = 20.8 \pm 0.2$   $\mu M$ ), on the other  
676 hand **2i** ( $IC_{50} = 17.3 \pm 0.1$   $\mu M$ ). This order is proportion to the noted biological activity. In overall,  
677 this result supports the experimental trend.

678

679 **Fig. 9.** HOMO, LUMO orbitals and their energy gap ( $\Delta E$  gap) of the compounds **2c** and **2i** at  
680 B3LYP/6-311++G (d, p) level of DFT.

681

682 For good absorption and permeability, the molecules must satisfy the Lipinski rules [91]. The rule  
683 describes the important molecular properties for a drug pharmacokinetics in the human body,  
684 including their absorption, distribution, metabolism and excretion. Lipinski's rule states that,  $\text{LogP} \leq 5$ ,  
685 molecular weight (MW)  $\leq 500$  Da, H-bond donors (HBD)  $\leq 5$  and H-bond acceptors (HBA)  $\leq$   
686 10.

687 The lipophilicity is proportional to the hydrophobic character of the substituent group [92]. The  
688  $\text{LogP}$  is the most useful parameter for the characterization of hydrophobicity (and polarity) of  
689 compounds. It is an important variable in QSAR studies because the distribution of chemicals  
690 between fatty and aqueous phases of a biological system could totally account for the variation in  
691 activities. A positive value for  $\text{logP}$  denotes a higher concentration in the lipid phase.

692 A drug targeting the central nervous system (CNS) should ideally have a logP value around 2 for  
693 oral and intestinal absorption the idea value is 1.35–1.8, while a drug intended for sub-lingual  
694 absorption should have a logP value >5. All our compounds respect this rule [93].

695 Table 4 reveals logP (3.53-0.23), compound **2f** (6-bromo-3-((3-(4-(tert-butyl)phenyl)isoxazol-5-  
696 yl)methoxy)-2-(4-(trifluoromethyl)phenyl)-4H-chromen-4-one, R<sub>1</sub>= tert-butyle, R<sub>2</sub>= H) has high  
697 value of logP (3.53). This compound generally has a good intestinal absorption owing to a good  
698 balance between solubility and passive diffusion permeability. In fact, the metabolism is minimized  
699 because of the lower binding with metabolic enzymes.

700 The most active compounds (**2b**, **2i**, **2k** and **2m**) have logP value (1.62, 2.43, 1 and 0.23,  
701 respectively). They are very lipophilic. Therefore, they have a good permeability through biological  
702 membrane, a better binding to plasma proteins, elimination by metabolism but a poor solubility.

703 Lipophilic ligand efficiency (LipE) is defined as: LipE = pIC<sub>50</sub> – logP. As a rough guide, medicinal  
704 compounds in drug-like space have LipE values in the range 2-7. Compound **2m** (6-bromo-3-((3-  
705 (3,4-dimethoxyphenyl)isoxazol-5-yl)methoxy)-2-(4-(trifluoromethyl)phenyl)-4H-chromen-4-one,  
706 R<sub>1</sub>= OCH<sub>3</sub>, R<sub>2</sub>= OCH<sub>3</sub>) has the highest LipE value (4.50) and it is deemed to be the most optimal  
707 compound (Table 4).

708 Lipinski's rule states that, LogP ≤ 5, molecular weight (MW) ≤ 500 Da, H-bond donors (HBD) ≤ 5  
709 and H-bond acceptors (HBA) ≤ 10. If molecules violating more than one of these parameters, they  
710 can have problems with bioavailability and high probability of failure to display drug-likeness.

711 Therefore, the obtained results reveal that the thirteen halogenated flavonoid-based isoxazole  
712 compounds respect the Lipinski rules except for the rule relating to molecular mass molecular  
713 weight (MW) ≤ 500 Da. Indeed, when the molecular weight is less than 500 Da it can be easily  
714 transported, diffused and absorbed through the cell membrane compared to heavy molecules. All  
715 selected compounds have (MW) > 500 Da. However, in 2014, Doak et al. [94] shown that strict  
716 reliance on the rule of 5 (Ro5) may have resulted in lost opportunities, particularly for difficult

717 targets. To identify opportunities for oral drug discovery beyond the Ro5 (bRo5), they have  
718 comprehensively analyzed drugs and clinical candidates with molecular weight (MW) > 500 Da.  
719 They conclude that oral drugs are found far bRo5 and properties such as intramolecular hydrogen  
720 bonding, macrocyclization, dosage and formulations can be used to improve bioavailability.  
721 Therefore, it suggested that these compounds do not have any problems with oral bioavailability.

722

#### 723 **Table 4**

724 Values of chemical descriptors used in the regression analysis. The energies of the HOMO ( $E_{\text{HOMO}}$ ,  
725 eV) and LUMO ( $E_{\text{LUMO}}$ , eV), energy gap ( $\Delta E$ , eV), hardness ( $\eta$ , eV), softness, ( $S$ , eV), potential ( $\mu$ ,  
726 eV), electrophilicity ( $\omega$ , eV) octanol-water partition coefficient ( $\log P$ ), polarizability ( $\text{Pol}$ ,  $\text{\AA}^3$ ),  
727 molar refractivity ( $\text{MR}$ ,  $\text{\AA}^3$ ), volume ( $V$ ,  $\text{\AA}^3$ ), surface area ( $\text{SAG}$ ,  $\text{\AA}^2$ ), molar weight ( $\text{MW}$ , amu).  
728 HBA and HBD are the numbers of the hydrogen bond acceptor and donor sites.

729

#### 730 **Conclusion**

731 In summary, this work reported a design and synthesis of new molecules described as halogenated  
732 flavonoid-based isoxazoles. Chemical structures were established by  $^1\text{H}$  NMR,  $^{13}\text{C}$  NMR and  
733 HRMS analysis. The obtained compounds were evaluated for their  $\alpha$ -amylase inhibitory activities  
734 and excellent results were noted. In addition, analysis of the structure-activity relationship revealed  
735 that alkoxyated and halogenated derivatives were found to be the most active compounds. Based  
736 on the *in silico* docking analysis, the halogenated flavonoid-based isoxazoles showed low binding  
737 energies, a large number of interactions and correct binding poses in the active pocket of the target  
738 enzyme. In addition, all the synthesized cycloadducts were modeled by DFT calculations using 6-  
739 311++G (d,p) basis set. The chemical stability, electrical transport properties, the geometrical  
740 parameters and frontier molecular orbitals of the halogenated flavonoid-based isoxazoles **2a-m**  
741 were determined and analyzed. Quantitative effects of the molecular structure of the cycloadducts

742 **2a-m** on their  $\alpha$ -amylase inhibitory activity were found. The obtained results made it possible to  
743 conclude that the newly synthesized compounds have no problem of oral bioavailability. These  
744 hybrid molecules can be considered as promising candidates for investigating new anti-obesity  
745 agents and antidiabetics.

746

#### 747 **Acknowledgments**

748 The authors express their thanks to the Ministry of Higher Education and Scientific Research of  
749 Tunisia for financial support (LR11ES39).

750

751 **Conflicts of Interest:** The authors declare no conflict of interest.

752

#### 753 **References**

- 754 [1] A. Boutayeb, S. Boutayeb, The burden of non communicable diseases in developing countries, *Int. J.*  
755 *Equity Health* 4 (2005) 1-8.
- 756 [2] K.H. Wagner, H. Brath, A global view on the development of non communicable diseases, *Prev.*  
757 *Med.* 54 (2012) S38-S41.
- 758 [3] P.M. Sales, P.M. Souza, L.A. Simeoni, P.O. Magalhães, D. Silveira,  $\alpha$ -Amylase inhibitors: a review  
759 of raw material and isolated compounds from plant source, *J. Pharm. Pharm. Sci.* 15 (2012) 141-183.
- 760 [4] S. Jayaraj, S. Suresh, R.K. Kadeppagari, Amylase inhibitors and their biomedical  
761 applications, *Starch-Stärke* 65 (2013) 535-542.
- 762 [5] S. Khan, M. Nazir, N. Raiz, M. Saleem, G. Zengin, G. Fazal, H. Saleem, M. Mukhtar, M.I. Tousif,  
763 R.B. Tareen, H.H. Abdallah, F.M. Mahomoodally, Phytochemical profiling, *in vitro* biological  
764 properties and in silico studies on *Caragana ambigua* stocks (Fabaceae): A comprehensive  
765 approach, *Ind. Crops Prod.* 131 (2019) 117-124.



- 766 [6] M. Kanwal, K.M. Khan, S. Chigurupati, F. Ali, M. Younus, M. Aldubayan, A. Wadood, H. Khan, M.  
767 Taha, S. Perveen, Indole-3-acetamides: As Potential Antihyperglycemic and Antioxidant Agents;  
768 Synthesis, *In Vitro*  $\alpha$ -Amylase Inhibitory Activity, Structure–Activity Relationship, and *In Silico*  
769 Studies, ACS omega 6 (2021) 2264-2275.
- 770 [7] A.M. Brzozowski, G.J. Davies, Structure of the *Aspergillus oryzae*  $\alpha$ -amylase complexed with the  
771 inhibitor acarbose at 2.0 Å resolution, Biochemistry 36 (1997) 10837-10845.
- 772 [8] P.M.D. Souza, P.D.O.E. Magalhães, Application of microbial  $\alpha$ -amylase in industry-A review, Braz.  
773 J. Microbiol. 41 (2010) 850-861.
- 774 [9] D. Malešev, V. Kuntić, Investigation of metal-flavonoid chelates and the determination of flavonoids  
775 via metal-flavonoid complexing reactions, J. Serb. Chem. Soc. 72 (2007) 921-939.
- 776 [10] P.F. Pinheiro, G.C. Justino, Structural analysis of flavonoids and related compounds - A review of  
777 spectroscopic applications, ISBN (2012) 978-953.
- 778 [11] J. Bruneton, Pharmacognosie, phytochimie, plantes médicinales (4e éd.). Lavoisier, 2009.
- 779 [12] E. Lo Piparo, H. Scheib, N. Frei, G. Williamson, M. Grigorov, C.J. Chou, Flavonoids for controlling  
780 starch digestion: structural requirements for inhibiting human  $\alpha$ -amylase, J. Med. Chem. 51 (2008)  
781 3555-3561.
- 782 [13] P.V.A. Babu, D. Liu, E. R. Gilbert, Recent advances in understanding the anti-diabetic actions of  
783 dietary flavonoids, J. Nutr. Biochem. 24 (2013) 1777-1789.
- 784 [14] R. Vinayagam, B. Xu, Antidiabetic properties of dietary flavonoids: a cellular mechanism review,  
785 Nutr. Metab. 12 (2015) 1-20.
- 786 [15] A. Ghorbani, Mechanisms of antidiabetic effects of flavonoid rutin, Biomed. Pharmacother. 96  
787 (2017) 305-312.
- 788 [16] L. Bai, X. Li, L. He, Y. Zheng, H. Lu, J. Li, L. Zhong, R. Tong, Z. Jiang, J. Shi, J. Li, Antidiabetic  
789 potential of flavonoids from traditional Chinese medicine: A review. Am. J. Chinese Med. 47 (2019)  
790 933-957.

- 791 [17] N.F. Brás, R.P. Neves, F.A. Lopes, M.A. Correia, A.S. Palma, S.F. Sousa, M.J. Ramos, Combined *in*  
792 *silico* and *in vitro* studies to identify novel antidiabetic flavonoids targeting glycogen  
793 phosphorylase, *Bioorg. Chem.* 108 (2021) 104552.
- 794 [18] J., Xiao, X., Ni, G., Kai, X., Chen, A review on structure-activity relationship of dietary polyphenols  
795 inhibiting  $\alpha$ -amylase, *Crit. Rev. Food Sci. Nutr.* 53 (2013) 497-506.
- 796 [19] F. Hua, P. Zhou, H.Y. Wu, G.X. Chu, Z.W. Xie, G.H. Bao, Inhibition of  $\alpha$ -glucosidase and  $\alpha$ -  
797 amylase by flavonoid glycosides from Lu'an GuaPian tea: molecular docking and interaction  
798 mechanism, *Food Funct.* 9 (2018) 4173-4183.
- 799 [20] L.P. Balant, M. Wermeille, Metabolism and pharmacokinetics of hydroxyethylated rutosides in  
800 animals and man. *Drug Metabol. Drug Interact.* 5 (1984) 1-24.
- 801 [21] P. Knekt, R. Jarvinen, A. Reunanen, J. Maatela, Flavonoid intake and coronary mortality in Finland:  
802 a cohort study, *Bmj* 312 (1996) 478-481.
- 803 [22] G. Di Carlo, N. Mascolo, A.A. Izzo, F. Capasso, Flavonoids: old and new aspects of a class of  
804 natural therapeutic drugs, *Life Sci.* 65 (1999) 337-353.
- 805 [23] P.G. Pietta, Flavonoids as antioxidants, *J. Nat. Prod.* 63 (2000) 1035-1042.
- 806 [24] A. García-Lafuente, E. Guillamón, A. Villares, M.A. Rostagno, J.A. Martínez, Flavonoids as anti-  
807 inflammatory agents: implications in cancer and cardiovascular disease, *Inflamm. Res.* 58 (2009)  
808 537-552.
- 809 [25] D. Lamoral-Theys, L. Pottier, F. Dufrasne, J. Nève, J. Dubois, A. Kornienko, R. Kiss, L. Ingrassia,  
810 Natural Polyphenols that Display Anticancer Activity through Inhibition of Kinase Activity, *Curr.*  
811 *Med. Chem.* 17 (2010) 812-825.
- 812 [26] N.G. Amado, B.F. Fonseca, D.M. Cerqueira, V.M. Neto, J.G. Abreu, Flavonoids: potential Wnt/beta-  
813 catenin signaling modulators in cancer, *Life Sci.* 89 (2011) 545-554.
- 814 [27] M.C.D.S. dos Santos, C.F.L. Gonçalves, M. Vaisman, A.C.F. Ferreira, D.P. de Carvalho, Impact of  
815 flavonoids on thyroid function, *Food Chem. Toxicol.* 49 (2011) 2495-2502.

- 816 [28] D. Dauzonne, B. Folléas, L. Martinez, G.G. Chabot, Synthesis and *in vitro* cytotoxicity of a series of  
817 3-aminoflavones, *Eur. J. Med. Chem.* 32 (1997) 71-82.
- 818 [29] G. Griebel, G. Perrault, S. Tan, H. Schoemaker, D.J. Sanger, Pharmacological studies on synthetic  
819 flavonoids: comparison with diazepam, *Neuropharmacology* 38 (1999) 965-977.
- 820 [30] S. Gunduz, A.C. Goren, T. Ozturk, Facile syntheses of 3-hydroxyflavones, *Org. Lett.* 14 (2012)  
821 1576-1579.
- 822 [31] E. Venkateswararao, M.J. Son, N. Sharma, M. Manickam, P. Boggu, Y.H. Kim, S.H. Woo, S.H.  
823 Jung, Exploration of pharmacophore in chryso splenol C as activator in ventricular myocyte  
824 contraction, *ACS Med. Chem. Lett.* 6 (2015) 758-763.
- 825 [32] M. Znati, C. Bordes, V. Forquet, P. Lantéri, H. Ben Jannet, J. Bouajila, Synthesis, molecular  
826 properties, anti-inflammatory and anticancer activities of novel 3-hydroxyflavone  
827 derivatives, *Bioorg. Chem.* 89 (2019) 103009.
- 828 [33] M. Duhan, R. Singh, M. Devi, J. Sindhu, R. Bhatia, A. Kumar, P. Kumar, Synthesis, molecular  
829 docking and QSAR study of thiazole clubbed pyrazole hybrid as  $\alpha$ -amylase inhibitor, *J. Biomol.*  
830 *Struct. Dyn.* 39 (2021) 91-107.
- 831 [34] H. Song, Research progress on trifluoromethyl-based radical reaction process, *IOP Conf. Ser.: Earth*  
832 *Environ. Sci.* 100 (2017) 012061.
- 833 [35] O.C. Agbaje, O.O. Fadeyi, S.A. Fadeyi, L.E. Myles, C.O. Okoro, Synthesis and *in vitro* cytotoxicity  
834 evaluation of some fluorinated hexahydropyrimidine derivatives, *Bioorg. Med. Chem. Lett.* 21  
835 (2011) 989-992.
- 836 [36] F. Xu, Y. Xia, Z. Feng, W. Lin, Q. Xue, J. Jiang, X. Yu, C. Peng, M. Luo, Y. Yang, Y. Wei, L. Yu,  
837 Repositioning antipsychotic fluphenazine hydrochloride for treating triple negative breast cancer with  
838 brain metastases and lung metastases, *Am. J. Cancer Res.* 9 (2019) 459-478.

- 839 [37] T. Ogawa, M. Inazu, K. Gotoh, T. Inoue, S. Hayashi, Therapeutic effects of leflunomide, a new  
840 antirheumatic drug, on glomerulonephritis induced by the antibasement membrane antibody in  
841 rats, *Clin. Immunol. Immunopathol.* 61 (1991) 103-118.
- 842 [38] P.L. McCormack, Celecoxib, *Drugs* 71 (2011) 2457-2489.
- 843 [39] P. Benfield, R.C. Heel, S.P. Lewis, Fluoxetine, *Drugs* 32 (1986) 481-508.
- 844 [40] A. Draper, P. Cullinan, C. Campbell, M. Jones, A.N. Taylor, Occupational asthma from fungicides  
845 fluazinam and chlorothalonil, *Occup. Environ. Med.* 60 (2003) 76-77.
- 846 [41] M. Nawaz, M. Taha, F. Qureshi, N. Ullah, M. Selvaraj, S. Shahzad, S. Chigurupati, A. Waheed, F.A.  
847 Almutairi, Structural elucidation, molecular docking,  $\alpha$ -amylase and  $\alpha$ -glucosidase inhibition studies  
848 of 5-amino-nicotinic acid derivatives, *BMC Chem.* 14 (2020) 43.
- 849 [42] H.R. Olpe, W.P. Koella, The action of muscimol on neurones of the substantia nigra of the  
850 rat, *Experientia* 34 (1978) 235-235.
- 851 [43] R. Schwarcz, T. Hökfelt, K. Fuxe, G. Jonsson, M. Goldstein, L. Terenius, Ibotenic acid-induced  
852 neuronal degeneration: a morphological and neurochemical study, *Exp. Brain Res.* 37 (1979) 199-  
853 216.
- 854 [44] M.C. Gennaro, D. Giacosa, E. Giannini, S. Angelino, Hallucinogenic species in *Amanita muscaria*.  
855 Determination of muscimol and ibotenic acid by ion-interaction HPLC, *J. Liq. Chromatogr. Relat.*  
856 *Technol.* 20 (1997) 413-424.
- 857 [45] S. Alaoui, M. Driowya, L. Demange, R. Benhida, K. Bougrin, Ultrasound-assisted facile one-pot  
858 sequential synthesis of novel sulfonamide-isoxazoles using cerium (IV) ammonium nitrate (CAN) as  
859 an efficient oxidant in aqueous medium, *Ultrason. Sonochem.* 40 (2018) 289-297.
- 860 [46] N.A. Nussmeier, A.A. Whelton, M.T. Brown, R.M. Langford, A. Hoeft, J.L. Parlow, S.W. Boyce,  
861 K.M. Verburg, Complications of the COX-2 inhibitors parecoxib and valdecoxib after cardiac  
862 surgery, *N. Engl. J. Med.* 352 (2005) 1081-1091.

- 863 [47] R. Yano, H. Yokoyama, H. Kuroiwa, H. Kato, T. Araki, A novel anti-Parkinsonian agent,  
864 zonisamide, attenuates MPTP-induced neurotoxicity in mice, *J. Mol. Neurosci.* 39 (2009) 211-219.
- 865 [48] A. Sysak, B. Obmińska-Mrukowicz, Isoxazole ring as a useful scaffold in a search for new  
866 therapeutic agents, *Eur. J. Med. Chem.* 137 (2017) 292-309.
- 867 [49] R. Sutherland, E.A.P. Croydon, G.N. Rolinson, Flucloxacillin, a new isoxazolyl penicillin, compared  
868 with oxacillin, cloxacillin, and dicloxacillin, *Br. Med. J.*, 4 (1970) 455-460.
- 869 [50] Y.S. Lee, B.H. Kim, Heterocyclic nucleoside analogues: design and synthesis of antiviral, modified  
870 nucleosides containing isoxazole heterocycles, *Bioorg. Med. Chem. Lett.* 12 (2002) 1395-1397.
- 871 [51] R.M. Kumbhare, U.B. Kosurkar, M.J. Ramaiah, T.L. Dadmal, S.N.C.V.L. Pushpavalli, M. Pal-  
872 Bhadra, Synthesis and biological evaluation of novel triazoles and isoxazoles linked 2-phenyl  
873 benzothiazole as potential anticancer agents, *Bioorg. Med. Chem. Lett.* 22 (2012) 5424-5427.
- 874 [52] S. Kankala, R.K. Kankala, P. Gundepaka, N. Thota, S. Nerella, M.R. Gangula, H. Guguloth, M.  
875 Kagga, R. Vadde, C.S. Vasam, Regioselective synthesis of isoxazole–mercaptobenzimidazole  
876 hybrids and their in vivo analgesic and anti-inflammatory activity studies, *Bioorg. Med. Chem. Lett.*  
877 23 (2013) 1306-1309.
- 878 [53] K. Chouaïb, A. Romdhane, S. Delemasure, P. Dutartre, N. Elie, D. Touboul, H. Ben Jannet, M.A.  
879 Hamza, Regiospecific synthesis, anti-inflammatory and anticancer evaluation of novel 3,5-  
880 disubstituted isoxazoles from the natural maslinic and oleanolic acids, *Ind. Crops Prod.* 85 (2016)  
881 287-299.
- 882 [54] J.P. Nie, Z.N. Qu, Y. Chen, J.H. Chen, Y. Jiang, M.N. Jin, Y. Yu, W.Y. Niu, H.Q. Duan, N. Qin,  
883 Discovery and anti-diabetic effects of novel isoxazole based flavonoid derivatives, *Fitoterapia* 142  
884 (2020) 104499.
- 885 [55] S. Chortani, M. Horchani, M. Znati, N. Issaoui, H. Ben Jannet, A. Romdhane, Design and synthesis  
886 of new benzopyrimidinone derivatives:  $\alpha$ -amylase inhibitory activity, molecular docking and DFT  
887 studies, *J. Mol. Struct.* 1230 (2021) 129920.

- 888 [56] <http://www.filefacts.com/acd3d-viewer-freeware-info>
- 889 [57] <https://www.rcsb.org>
- 890 [58] O. Trot, A.J. Olson, AutoDock Vina: improving the speed and accuracy of docking with a new  
891 scoring function, efficient optimization, and multithreading, *J. Comput. Chem.* 31 (2010) 455-461.
- 892 [59] M.J. Frisch, G.W. Trucks, H.B. Schlegel, G.E. Scuseria, M.A. Robb, J.R. Cheeseman, G. Scalmani,  
893 V. Barone, B. Mennucci, G.A. Petersson, H. Nakatsuji, M. Caricato, X. Li, H.P. Hratchian, A.F.  
894 Izmaylov, J. Bloino, G. Zheng, J.L. Sonnenberg, M. Hada, M. Ehara, K. Toyota, R. Fukuda, J.  
895 Hasegawa, M. Ishida, T. Nakajima, Y. Honda, O. Kitao, H. Nakai, T. Vreven, J.A. Montgomery,  
896 Jr.J.E. Peralta, F. Ogliaro, M. Bearpark, J.J. Heyd, E. Brothers, K.N. Kudin, V.N. Staroverov, R.  
897 Kobayashi, J. Normand, K. Raghavachari, A. Rendell, J.C. Burant, S.S. Iyengar, J. Tomasi, M. Cossi,  
898 N. Rega, J.M. Millam, M. Klene, J.E. Knox, J.B. Cross, V. Bakken, C. Adamo, J. Jaramillo, R.  
899 Gomperts, R.E. Stratmann, O. Yazyev, A.J. Austin, R. Cammi, C. Pomelli, J.W. Ochterski, R.L.  
900 Martin, K. Morokuma, V.G. Zakrzewski, G.A. Voth, P. Salvador, J.J. Dannenberg, S. Dapprich, A.D.  
901 Daniels, Ö. Farkas, J.B. Foresman, J.V. Ortiz, J. Cioslowski, D.J. Fox, Gaussian 09, Revision A. 02,  
902 Gaussian Inc., Wallingford, CT, 2009
- 903 [60] A.D. Becke, Density-Functional Thermochemistry. III. The Role of Exact Exchange, *J. Chem. Phys.*  
904 98 (1993) 5648-5652.
- 905 [61] S. Grimme, S. Ehrlich, L. Goerigk, Effect of the damping function in dispersion corrected density  
906 functional theory, *J. Comp. Chem.* 32 (2011) 1456–1465.
- 907 [62] C. Lee, W. Yang, R.G. Parr, Development of the Colle-Salvetti correlation-energy formula into a  
908 functional of the electron density, *Phys. Rev. B.* 37 (1988) 785–789.
- 909 [63] R.T. Sanderson, Electronegativity and bond energy, *J. Am. Chem. Soc.* 105 (1983) 2259-2261.
- 910 [64] H. Schröder, A. Creon, T. Schwabe, Reformulation of the D3 (Becke–Johnson) dispersion correction  
911 without resorting to higher than C 6 dispersion coefficients, *J. Chem. Theory Comput.* 11 (2015)  
912 3163–3170.

- 913 [65] T. Koopmans, Ordering of wave functions and eigenenergies to the individual electrons of an atom.  
914 Physica, 1 (1933) 104-113.
- 915 [66] A.E. Reed, L.A. Curtiss, F. Weinhold, Intermolecular interactions from a natural bond orbital, donor-  
916 acceptor viewpoint, Chem. Rev. 88 (1988) 899-926.
- 917 [67] HyperChem (Molecular Modeling System), Hypercube, Inc., Gainesville, FL 32601, USA, 1115NW,  
918 2008.
- 919 [68] A. K. Ghose, G. M. Crippen, Atomic physicochemical parameters for three-dimensional-structure-  
920 directed quantitative structure-activity relationships. 2. Modeling dispersive and hydrophobic  
921 interactions, J. Chem. Inf. Comp. Sci. 27 (1987) 21-35.
- 922 [69] K.J. Miller, Additivity methods in molecular polarizability, J. Am. Chem. Soc. 112 (1990) 8533-  
923 8542.
- 924 [70] A. Gavezzotti, The calculation of molecular volumes and the use of volume analysis in the  
925 investigation of structured media and of solid-state organic reactivity, J. Am. Chem. Soc. 105 (1983)  
926 5220-5225.
- 927 [71] N. Bodor, Z. Gabanyi, C.K. Wong, A new method for the estimation of partition coefficient, J. Am.  
928 Chem. Soc. 111 (1989) 3783-3786.
- 929 [72] F. Himo, T. Lovell, R. Hilgraf, V.V. Rostovtsev, L. Noodleman, K.B. Sharpless, V.V. Fokin, Copper  
930 (I)-catalyzed synthesis of azoles. DFT study predicts unprecedented reactivity and intermediates, J.  
931 Am. Chem. Soc. 127 (2005) 210-216.
- 932 [73] G. Ak, G. Zengin, R. Ceylan, M.F. Mahomoodally, S. Jugreet, A. Mollica, A. Stefanucci, Chemical  
933 composition and biological activities of essential oils from *Calendula officinalis* L. flowers and  
934 leaves, Flavour Fragr. J. 00 (2021) 1-10.
- 935 [74] C. Placines, V. Castañeda-Loaiza, M. João Rodrigues, C.G. Pereira, A. Stefanucci, A. Mollica, G.  
936 Zengin, E.J. Llorent-Martínez, P.C. Castilho, L. Custódio, Phenolic profile, toxicity, enzyme

937 inhibition, *in silico* studies, and antioxidant properties of *Cakile maritima* scop.(Brassicaceae) from  
938 southern Portugal, *Plants* 9 (2020) 142.

939 [75] K.I. Sinan, O.K. Etienne, A. Stefanucci, A. Mollica, M.F. Mahomoodally, S. Jugreet, G. Rocchetti,  
940 L. Lucini, A. Aktumsek, D. Montesano, G. Ak, G. Zengin, Chemodiversity and biological activity of  
941 essential oils from three species from the *Euphorbia* genus, *Flavour Fragr. J.* 36 (2021) 148-158.

942 [76] I. Saidi, W. Baccari, A. Marchal, P. Waffo-Téguo, A.H. Harrath, L. Mansour, H. Ben Jannet, Iridoid  
943 glycosides from the Tunisian *Citharexylum spinosum* L.: Isolation, structure elucidation, biological  
944 evaluation, molecular docking and SAR analysis, *Ind. Crops Prod.* 151 (2020) 112440.

945 [77] I. Saidi, V.D. Nimbarte, H. Schwalbe, P. Waffo-Téguo, A.H. Harrath, L. Mansour, S. Alwasel, H.  
946 Ben Jannet, Anti-tyrosinase, anti-cholinesterase and cytotoxic activities of extracts and  
947 phytochemicals from the Tunisian *Citharexylum spinosum* L.: Molecular docking and SAR  
948 analysis, *Bioorg. Chem.* 102 (2020) 104093.

949 [78] <https://www.rcsb.org/structure/7TAA>

950 [79] M.L. Laury, M.J. Carlson, A.K., Wilson, Vibrational frequency scale factors for density functional  
951 theory and the polarization consistent basis sets, *J. Comput. Chem.* 33 (2012) 2380–2387.

952 [80] O. Prasad, L. Sinha, N. Kumar, Theoretical Raman and IR spectra of tegafur and comparison of  
953 molecular electrostatic potential surfaces, polarizability and hyperpolarizability of tegafur with 5-  
954 fluoro-uracil by density functional theory, *J. At. Mol. Sci.* 1 (2010) 201-214.

955 [81] R.K. Srivastava, V. Narayan, O. Prasad, L. Sinha, Vibrational, Structural and Electronic properties of  
956 6-methyl nicotinic acid by Density Functional Theory, *J. Chem. Pharm. Res.* 4 (2012) 3287-3296.

957 [82] J. Wang, X.Q. Xie, T. Hou, X. Xu, Fast approaches for molecular polarizability calculations, *J. Phys.*  
958 *Chem. A* 111 (2007) 4443-4448.

959 [83] H.A. Lorentz, *Collected papers*, Martinus Nijhoff, The Hague, 2 (1934–1936) 1–119.

960 [84] H. Kragh, The Lorenz-Lorentz formula: Origin and early history, *Substantia* 2 (2018) 7-18.



- 961 [85] H. Chermette, Chemical reactivity indexes in density functional theory, *J. Comp. Chem.* 20 (1999)  
962 129-154.
- 963 [86] J. Padmanabhan, R. Parthasarathi, U. Sarkar, V. Subramanian, P.K. Chattaraj, Effect of solvation on  
964 the condensed Fukui function and the generalized philicity index, *Chem. Phys. Lett.* 383 (2004) 122-  
965 128.
- 966 [87] R.G. Parr, W. Yang, Density functional approach to the frontier-electron theory of chemical  
967 reactivity, *J. Am. Chem. Soc.* 106 (1984) 4049-4050.
- 968 [88] R.G. Parr, R.G. Pearson, Absolute hardness: companion parameter to absolute electronegativity, *J.*  
969 *Am. Chem. Soc.* 105 (1983) 7512-7516.
- 970 [89] O. Nouredine, S. Gatfaoui, S.A. Brandán, H. Marouani, N. Issaoui, Structural, docking and  
971 spectroscopic studies of a new piperazine derivative, 1-Phenylpiperazine-1,4-dium bis(hydrogen  
972 sulfate, *J. Mol. Struct* 1212 (2020) 127351.
- 973 [90] M. Manachou, Z. Goud, Z. Almi, S. Belaidi, S. Boughdiri and M. Hochlaf, Pyrazolo[1,5-  
974 a][1,3,5]triazin-2-thioxo-4-ones derivatives as thymidine phosphorylase inhibitors: Structure, drug-  
975 like calculations and quantitative structureactivity relationships (QSAR) modeling, *J. Mol. Struct.*  
976 1199 (2020) 127027.
- 977 [91] C.A. Lipinski, F. Lombardo, B.W. Dominy, P. Feeny, Experimental and computational approaches  
978 to estimate solubility and permeability in drug discovery and development settings, *Adv. Drug Deliv.*  
979 *Rev.* 23 (1997) 3-25.
- 980 [92] H. Pajouhesh, G. R. Lenz, Medicinal chemical properties of successful central nervous system drugs.  
981 *NeuroRx* 2 (2005) 541-553.
- 982 [93] C. Hansch, J.P. Björkroth, A. Leo, Hydrophobicity and central nervous system agents: on the  
983 principle of minimal hydrophobicity in drug design, *J. Pharm. Sci.* 76 (1987) 663-687.
- 984 [94] B.C. Doak, B. Over, F. Giordanetto, J. Kihlberg, Oral druggable space beyond the rule of 5: insights  
985 from drugs and clinical candidates, *Chem. Biol.* 21 (2014) 1115-1142.

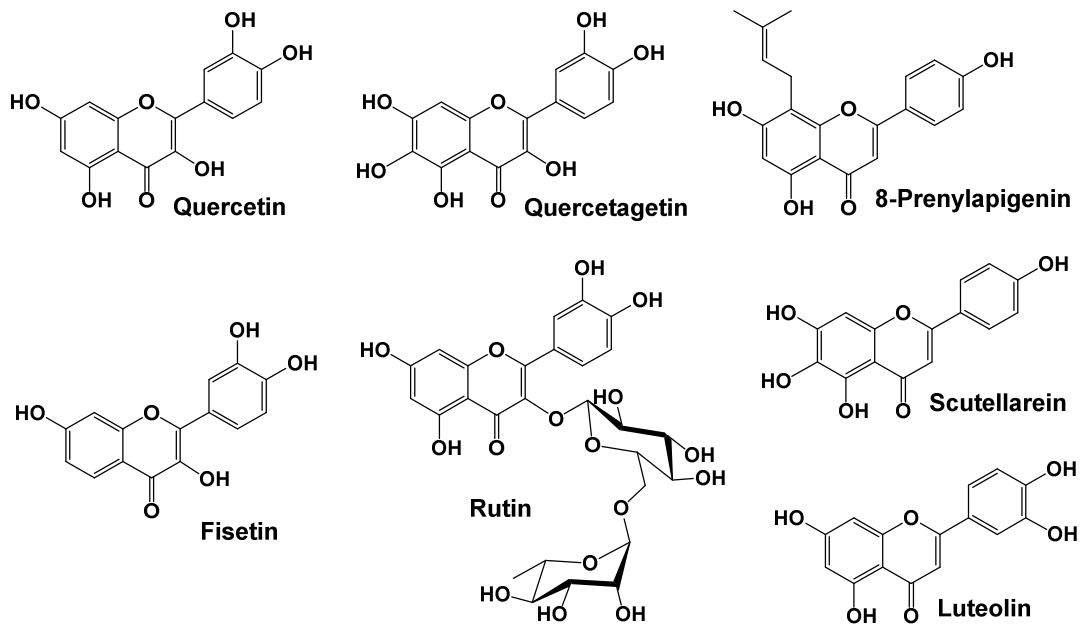


**Fig. 1.** Example of flavonoids previously reported as antidiabetics.

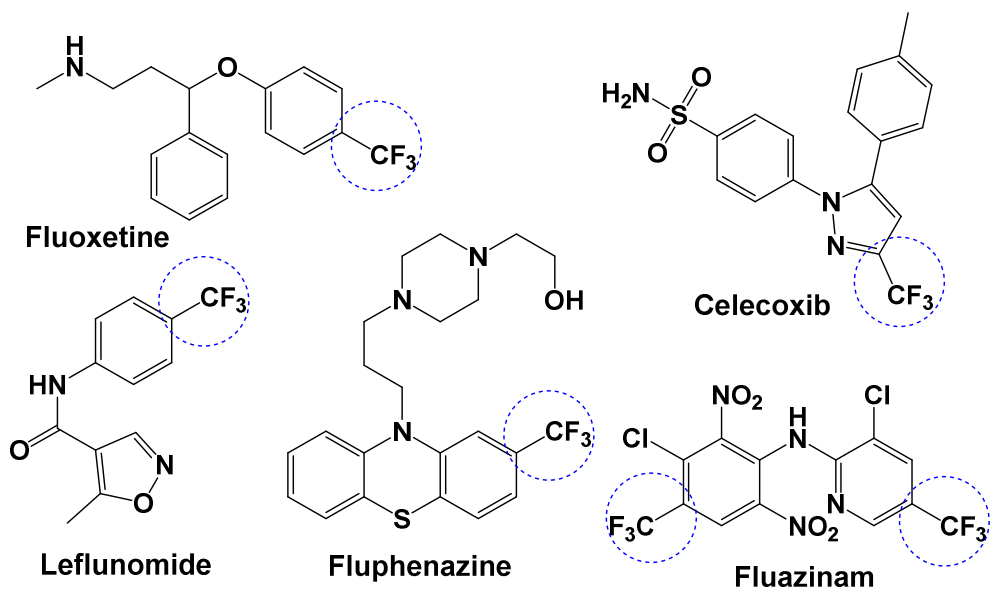


**Fig. 2.** Structures of trifluoromethylated drugs.

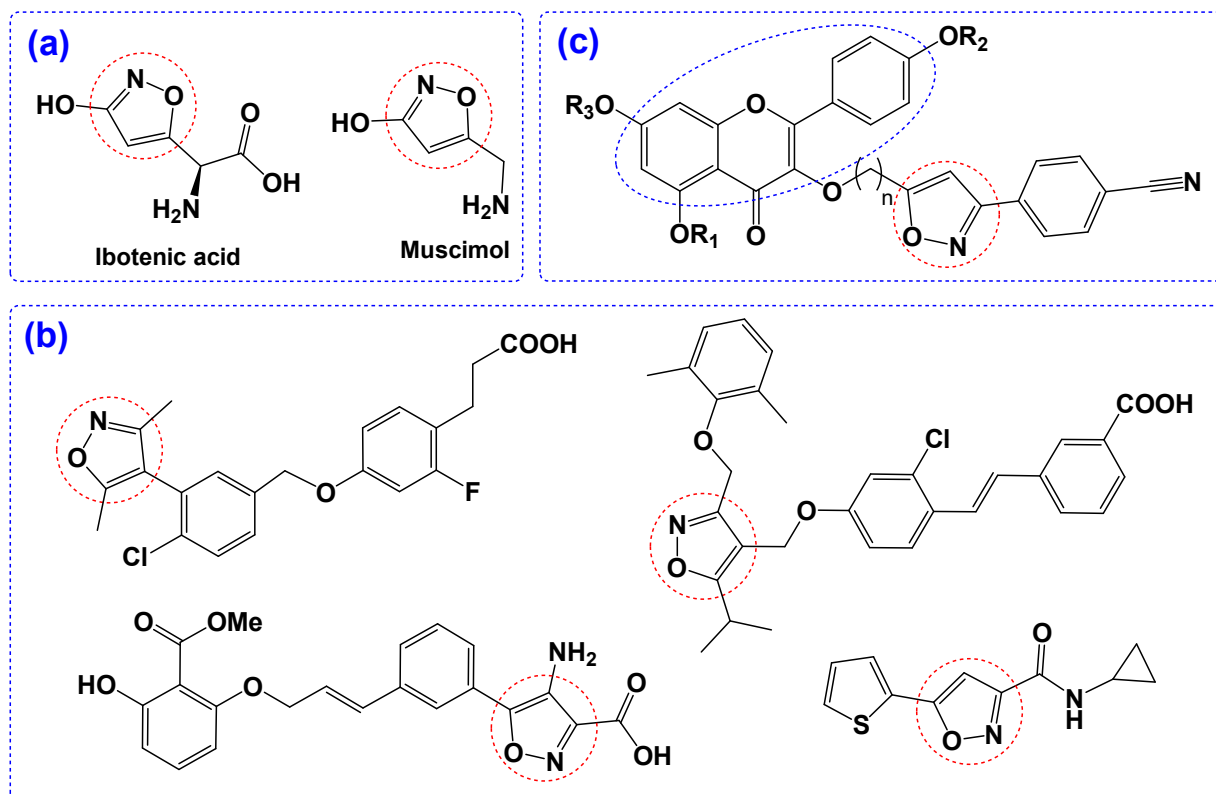


**Fig. 3.** (a) Natural compounds containing isoxazole ring (b) Previously reported isoxazole derivatives as antidiabetic agents (c) Reported flavonoid-based isoxazoles with antidiabetic properties.

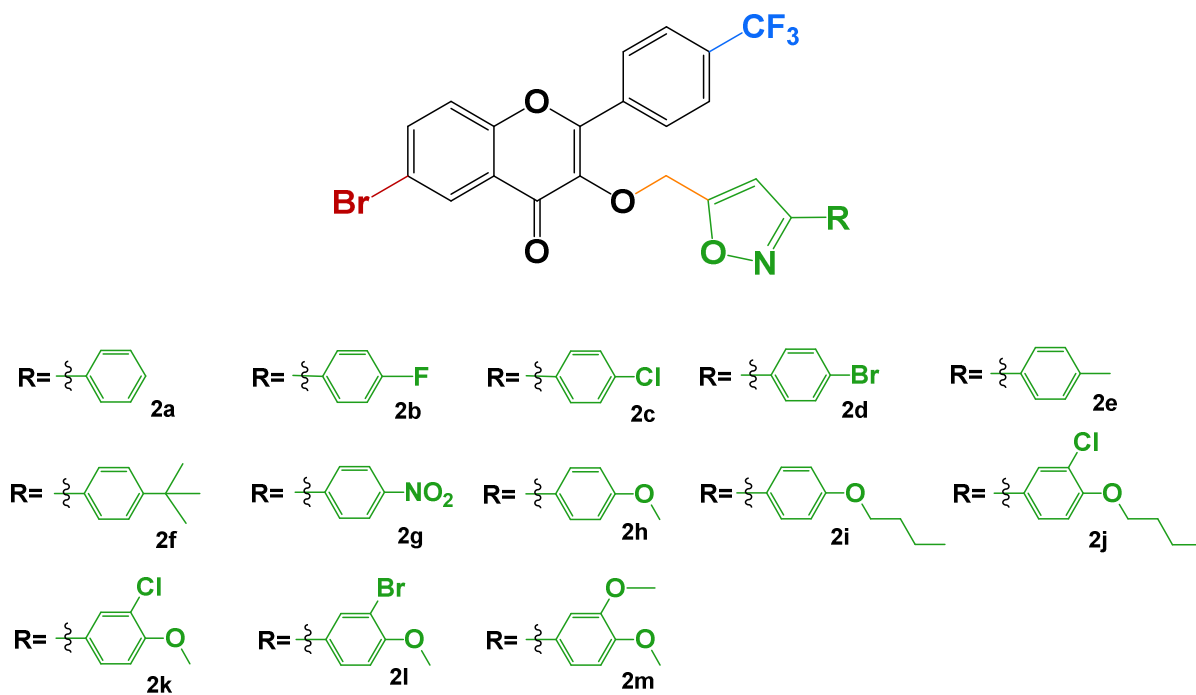


**Fig. 4.** Structures of halogenated flavonoid-based isoxazoles (**2a-m**).

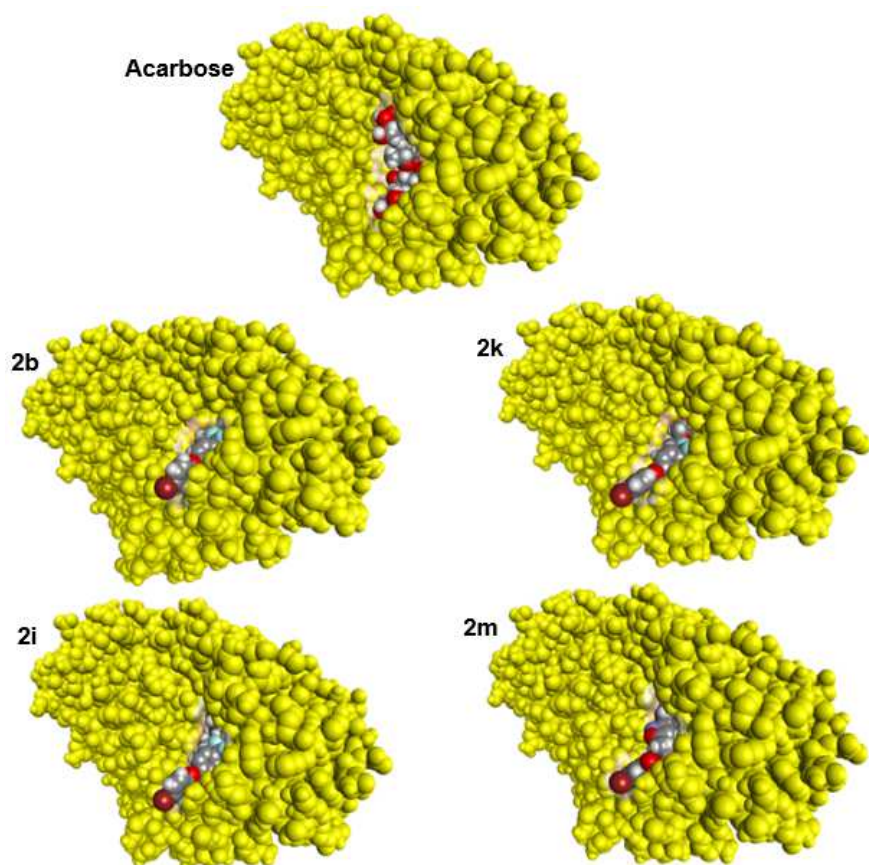


**Fig. 5.** The binding pose of acarbose, **2b**, **2i**, **2k** and **2m** in  $\alpha$ -amylase enzyme.

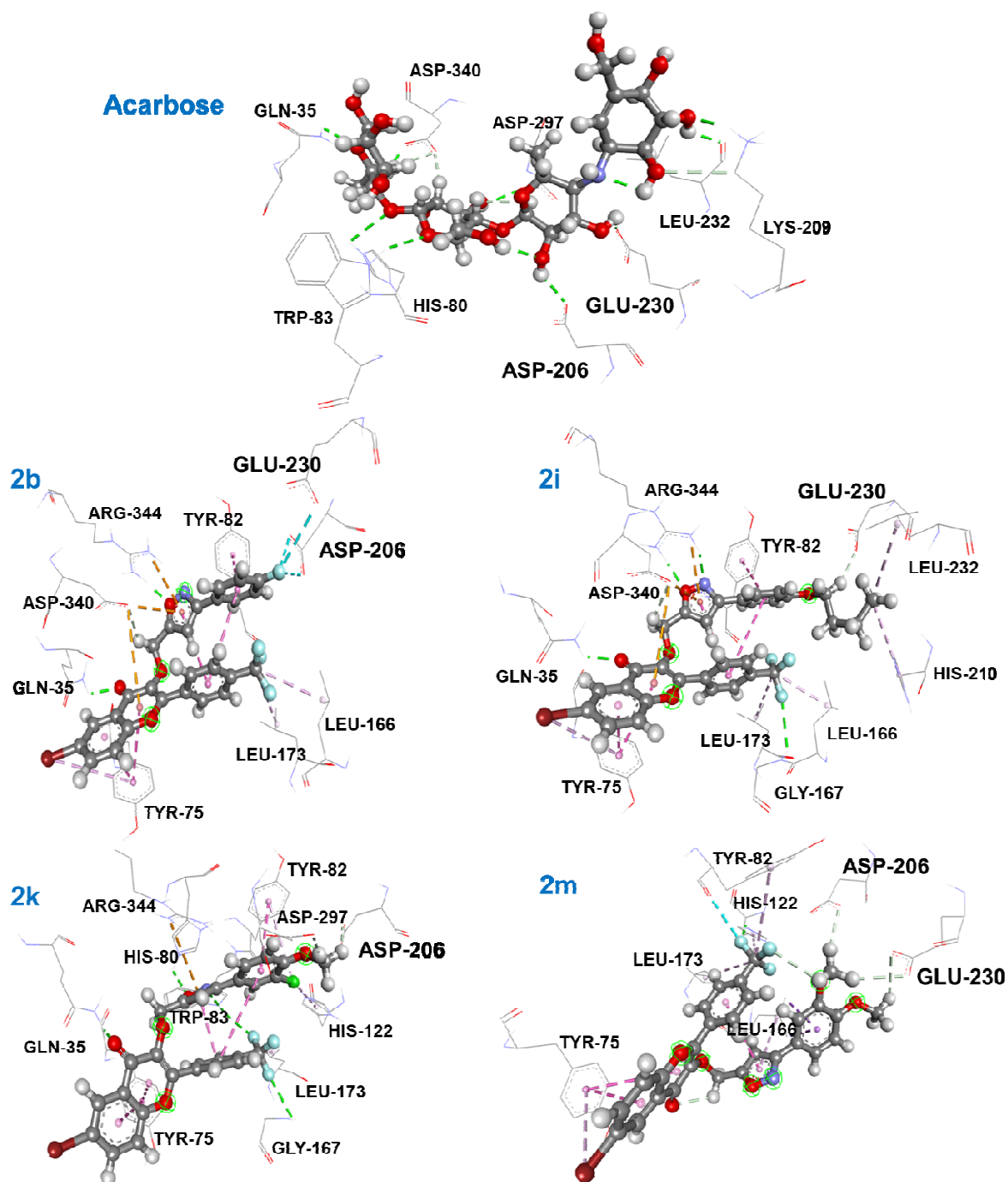


**Fig. 6.** Acarbose and compound **2b**, **2i**, **2k** et **2m** fits into the hydrophobic binding pocket of ABC in PDB: 7TAA.

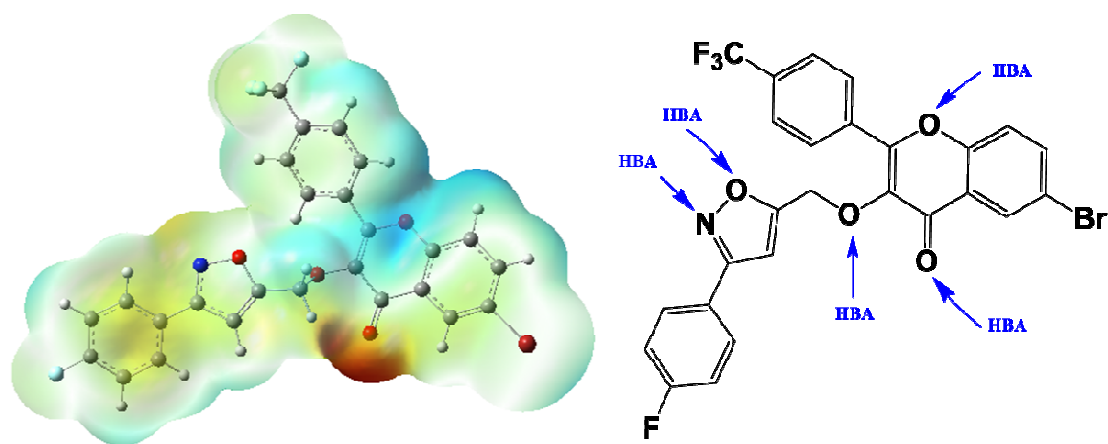


**Fig. 7.** 3D MESP surface map (left) for 6-bromo-3-((3-(4-fluorophenyl)isoxazol-5-yl)methoxy)-2-(4-(trifluoromethyl)phenyl)-4*H*-chromen-4-one (**2b**) and **its** hydrogen bond acceptor (HBA) sites (right). The red regions correspond to negative potentials and the blue regions to positive potentials.





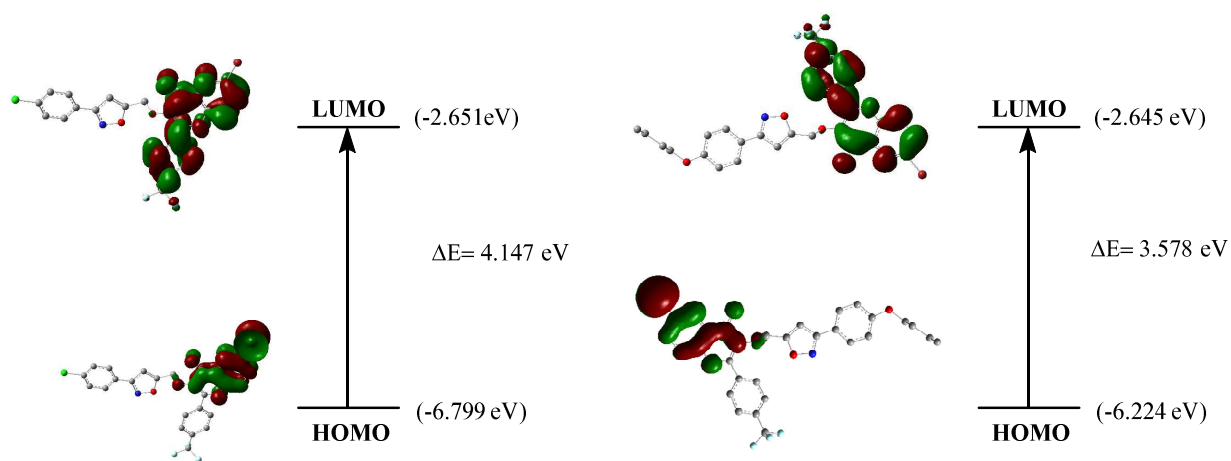


**Fig. 9.** HOMO, LUMO orbitals and their energy gap ( $\Delta E$  gap) of the compounds **2c** and **2i** at B3LYP/6-311++G (d, p) level of DFT.

**Table 1**

$\alpha$ -Amylase inhibition ( $IC_{50}$   $\mu$ M), binding energy (kcal/mol) and interaction detail of compounds **1**, **2** and **2a-m** docked in the ABC pocket (PDB: 7TAA).

Comp.	$\alpha$ -Amylase inhibition ( $IC_{50}$ $\mu$ M)	Binding energy (kcal/mol)	Interaction detail: NI/NIAA: IAA
<b>1</b>	21.47 $\pm$ 0.62	-7.5	10/6: GLN-35*, TYR-75, TYR-82, HIS-122*, <b>ASP-206</b> , ASP-340
<b>2</b>	24.32 $\pm$ 0.46	-7.6	14/9: TYR-75, HIS-80, TYR-82, TRP-83, HIS-210*, <b>GLU-230</b> , HIS-296, ASP-340, ARG-344
<b>2a</b>	33.15 $\pm$ 0.77	-9.3	9/7: GLN-35*, TYR-75, HIS-80, TYR-82, LEU-166, ASP-340, ARG-344*
<b>2b</b>	16.20 $\pm$ 0.31	-9.6	15/9 : GLN-35*, TYR-75, TYR-82, LEU-166, LEU-173, <b>ASP-206</b> , <b>GLU-230</b> , ASP-340, ARG-344*
<b>2c</b>	20.76 $\pm$ 0.19	-8.7	12/7 : HIS-80, TYR-82, TRP-83, TYR-155, LEU-166, GLY-167*, LEU-173, <b>ASP-206</b> , LEU-232, ASP-340
<b>2d</b>	21.17 $\pm$ 0.16	-8.3	14/8: TYR-75, TYR-82, HIS-122*, LEU-166, <b>ASP-206</b> , LYS-209, HIS-210, LEU-232
<b>2e</b>	32.80 $\pm$ 1.05	-9.5	12/8 : GLN-35*, TYR-75, TYR-82, LEU-166, LEU-173, ASP-297, ASP-340, ARG-344*
<b>2f</b>	33.26 $\pm$ 0.41	-8.5	12/9: GLN-35*, TYR-75, HIS-80, TYR-82, TRP-83, GLY-167*, LEU-173, ASP-340, ARG-344*
<b>2g</b>	24.71 $\pm$ 0.33	-8.6	11/11: GLN-35*, TYR-75, HIS-80, TYR-82, LEU-166, GLY-167*, LEU-173, ARG-204*, HIS-296*, ASP-340, PRO-341
<b>2h</b>	19.25 $\pm$ 0.39	-8.7	12/9: HIS-80*, TYR-82, LEU-166, GLY-167*, LEU-173, TYR-155, <b>ASP-206</b> , LEU-232, ASP-340
<b>2i</b>	17.33 $\pm$ 0.13	-9.3	17/11 : GLN-35*, TYR-75, TYR-82, LEU-166, GLY-167*, LEU-173, HIS-210, <b>GLU-230</b> , LEU-232, ASP-340, ARG-344**
<b>2j</b>	23.99 $\pm$ 0.29	-8.0	12/10: GLN-35*, TYR-75, TYR-82, TRP-83*, HIS-122, GLY-167*, LEU-173, ASP-297, PRO-341, ARG-344
<b>2k</b>	17.58 $\pm$ 0.26	-8.8	14/11: GLN-35*, TYR-75, HIS-80*, TYR-82, TRP-83**, HIS-122, GLY-167*, LEU-173, <b>GLU-230</b> , ASP-297, ARG-344
<b>2l</b>	30.86 $\pm$ 0.47	-9.4	13/8: GLN-35*, TYR-75, HIS-80, TYR-82, LEU-166, ASP-297, ASP-340, ARG-344**
<b>2m</b>	18.36 $\pm$ 0.14	-8.7	14/7 : TYR-75, TYR-82, HIS-122*, LEU-166, LEU-173, <b>ASP-206</b> , <b>GLU-230</b>
<b>Acarbose</b>	15.74 $\pm$ 0.21	-7.9	11/9: GLN-35*, HIS-80*, TRP-83*, <b>ASP-206*</b> , LYS-209*, <b>GLU-230*</b> , LEU-232*, ASP-297*, ASP-340*

NI: Number of interactions, NIAA: Number of interacting amino acids, IAA: Interacting amino acids, \*= One hydrogen bond, \*\*= Two hydrogen bonds.

**Table 2**

Anharmonic vibrational frequencies (in  $\text{cm}^{-1}$ ) of 6-bromo-3-((3-(4-fluorophenyl)isoxazol-5-yl)methoxy)-2-(4-(trifluoromethyl)phenyl)-4H-chromen-4-one as computed using B3LYP in conjunction with the 6-311++ G (d,p) basis set. Also their assignment was given.

Sym.	B3LYP	Assignment
a'	3179.1	C–H stretching
a'	3155.1	C–H stretching
a'	1606.0	C=C stretching
a'	1604.9	C=O stretching
a'	1443.9	C=N stretching
a'	1362.3	C–O stretching
a'	1271.3	N–O in-plane bending
a'	677.8	C–Br stretching
a'	967.6	N–O–C in-plane-bending
a'	661.5	Wagging C=O
a''	622.4	Molecule deformation in-plane-bending
a''	575.6	Molecule deformation in-plane-bending
a''	268.5	Rings deformation out-of-plane-bending
a''	227.4	Molecule deformation out-of-plane-bending
a''	201.1	Molecule deformation out-of-plane-bending

**Table 3**

Scaled anharmonic vibrational frequencies (in  $\text{cm}^{-1}$ ) (scaling factor 0.9662 [74]) of some elongation modes of flavonoid-based isoxazole derivatives as computed using B3LYP/6-311++G (d,p).

Comp.	C-O	C=O	C=N	O-N
<b>2a</b>	1363.0	1586.3	1424.3	1271.9
<b>2b</b>	1362.3	1604.9	1443.9	1271.3
<b>2c</b>	1362.6	1607.8	1442.2	1270.4
<b>2d</b>	1362.7	1607.7	1443.0	1271.7
<b>2e</b>	1362.4	1607.4	1454.1	1270.9
<b>2f</b>	1362.6	1605.9	1442.9	1272.3
<b>2g</b>	1362.5	1605.9	1443.5	1272.5
<b>2h</b>	1362.8	1607.7	1443.3	1272.1
<b>2i</b>	1363.5	1607.9	1444.0	1272.9
<b>2j</b>	1363.2	1607.7	1440.3	1271.2
<b>2k</b>	1363.1	1607.8	1441.3	1269.7
<b>2l</b>	1362.4	1607.5	1441.4	1270.4
<b>2m</b>	1363.0	1606.0	1438.1	1270.7

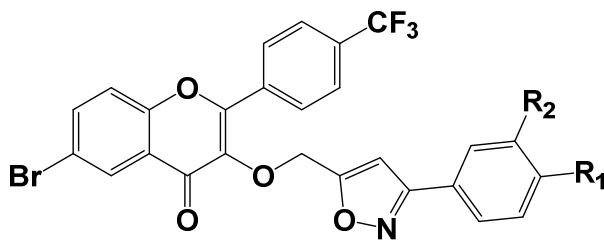
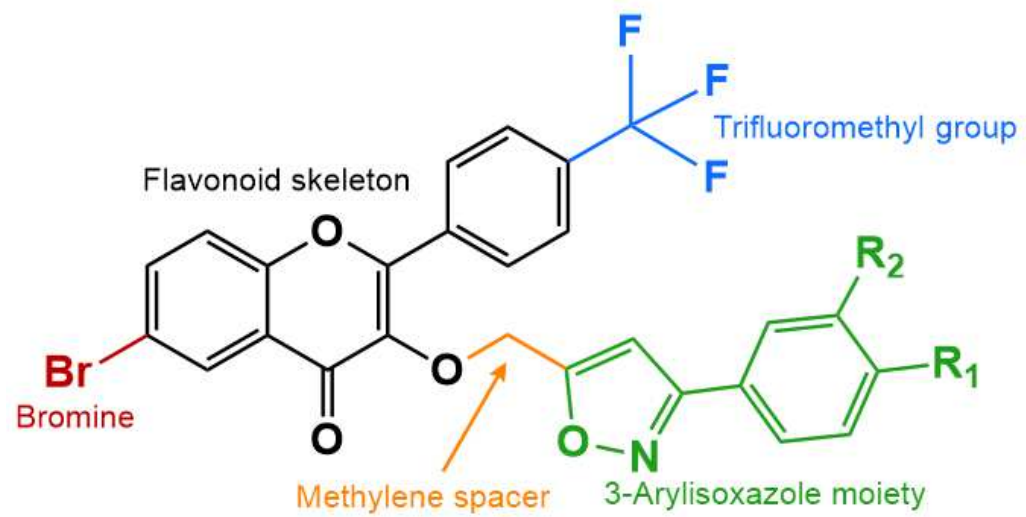


**Table 4**

Values of chemical descriptors used in the regression analysis. The energies of the HOMO ( $E_{\text{HOMO}}$ , eV) and LUMO ( $E_{\text{LUMO}}$ , eV), energy gap ( $\Delta E$ , eV), hardness ( $\eta$ , eV), softness, ( $S$ , eV), potential ( $\mu$ , eV), electrophilicity ( $\omega$ , eV) octanol-water partition coefficient (log P), polarizability (Pol,  $\text{\AA}^3$ ), molar refractivity (MR,  $\text{\AA}^3$ ), volume (V,  $\text{\AA}^3$ ), surface area (SAG,  $\text{\AA}^2$ ), molar weight (MW, amu). HBA and HBD are the numbers of the hydrogen bond acceptor and donor sites.

Comp.	PIC50*	LUMO	HOMO	$\Delta E$	S	$\mu$	$\eta$	$\omega$	LipE	LogP	MW	Pol	R	SAG	Vol	HBD	HBA
<b>2a</b>	4.479	-2.654	-6.785	4.131	0.242	-4.720	2.065	-5.393	2.259	2.22	542.31	47.79	140.54	715.55	1234.17	0	5
<b>2b</b>	4.790	-2.655	-6.798	4.142	0.241	-4.726	2.071	-5.393	3.170	1.62	560.30	47.70	140.67	720.80	1243.37	0	5
<b>2c</b>	4.682	-2.651	-6.799	4.147	0.241	-4.725	2.070	-5.383	2.682	2.00	576.75	49.71	145.26	750.2	1286.74	0	5
<b>2d</b>	4.674	-2.651	-6.786	4.135	0.241	-4.719	2.067	-5.385	2.404	2.27	621.20	50.41	148.07	754.11	1305.49	0	5
<b>2e</b>	4.484	-2.652	-6.686	4.033	0.247	-4.669	2.016	-5.405	2.114	2.37	556.34	49.62	144.82	751.15	1292.68	0	5
<b>2f</b>	4.478	-2.647	-6.686	4.039	0.247	-4.667	2.019	-5.392	0.948	3.53	598.42	55.13	158.45	819.07	1431.13	0	5
<b>2g</b>	4.607	-3.273	-6.807	3.533	0.283	-5.040	1.766	-7.189	3.207	1.40	587.31	49.50	146.76	752.84	1300.06	0	8
<b>2h</b>	4.715	-2.645	-6.293	3.648	0.274	-4.469	1.824	-5.475	3.485	1.23	572.33	50.26	146.92	765.39	1318.05	0	6
<b>2i</b>	4.761	-2.645	-6.224	3.578	0.279	-4.435	1.789	-5.496	2.331	2.43	614.42	55.76	160.79	849.52	1477.87	0	6
<b>2j</b>	4.619	-2.650	-6.791	4.140	0.241	-4.720	2.070	-5.383	2.409	2.21	648.86	57.69	165.50	869.93	1518.66	0	6
<b>2k</b>	4.754	-2.649	-6.795	4.145	0.241	-4.722	2.072	-5.379	3.754	1.00	606.78	52.19	151.63	783.73	1360.29	0	6
<b>2l</b>	4.510	-2.652	-6.789	4.137	0.241	-4.721	2.068	-5.386	2.230	1.28	542.31	47.79	140.54	715.55	1234.17	0	6
<b>2m</b>	4.736	-2.652	-6.565	3.913	0.255	-4.609	1.956	-5.428	4.506	0.23	560.30	47.70	140.67	720.80	1243.37	0	7

\*PIC50= -logIC50



- ✓ **Synthesis**
- ✓ ***In vitro* Inhibition of  $\alpha$ -Amylase Activity**
- ✓ **Structure-Activity Relationship Analysis**
- ✓ ***In silico* Docking and DFT Studies**

